



## Research



**Cite this article:** von der Gracht S, Nijholt E, Rink B. 2024 Higher-order interactions lead to 'reluctant' synchrony breaking. *Proc. R. Soc. A* **480**: 20230945.

<https://doi.org/10.1098/rspa.2023.0945>

Received: 21 December 2023

Accepted: 17 July 2024

**Subject Category:**

Mathematics

**Subject Areas:**

applied mathematics, differential equations

**Keywords:**

higher-order interactions, synchrony breaking, network dynamics, coupled cell systems

**Authors for correspondence:**

Sören von der Gracht

e-mail: [soeren.von.der.gracht@uni-paderborn.de](mailto:soeren.von.der.gracht@uni-paderborn.de)

Eddie Nijholt

e-mail: [eddie.nijholt@gmail.com](mailto:eddie.nijholt@gmail.com)

Electronic supplementary material is available online at <https://doi.org/10.6084/m9.figshare.c.7441723>.

# Higher-order interactions lead to 'reluctant' synchrony breaking

Sören von der Gracht<sup>1</sup>, Eddie Nijholt<sup>2</sup> and Bob Rink<sup>3</sup>

<sup>1</sup>Institute of Mathematics, Paderborn University, Warburger Straße 100, Paderborn 33098, Germany

<sup>2</sup>Department of Mathematics, Imperial College London, 180 Queen's Gate, London SW7 2AZ, UK

<sup>3</sup>Department of Mathematics, Faculty of Science, Vrije Universiteit Amsterdam, De Boelelaan 1111, Amsterdam 1081 HV, The Netherlands

SvdG, 0000-0002-8054-2058; EN, 0000-0001-5984-4572; BR, 0002-6695-8735

To model dynamical systems on networks with higher-order (non-pairwise) interactions, we recently introduced a new class of ordinary differential equations (ODEs) on hypernetworks. Here, we consider one-parameter synchrony breaking bifurcations in such ODEs. We call a synchrony breaking steady-state branch 'reluctant' if it is tangent to a synchrony space, but does not lie inside it. We prove that reluctant synchrony breaking is ubiquitous in hypernetwork systems, by constructing a large class of examples that support it. We also give an explicit formula for the order of tangency to the synchrony space of a reluctant steady-state branch.

## 1. Introduction

Recent advances in a large variety of research fields have highlighted the importance of non-pairwise interactions for the collective dynamical behaviour of complex network systems. These so-called higher-order interactions turn out to be crucial in problems from, e.g. neuroscience (see [1,2]), social science (see [3]) and ecology (see [4–6]). Physicists have, in particular, emphasized the impact of group interactions on synchronization behaviour in various coupled oscillator models and their generalizations (such as topological signals on cell complexes or swarmalators with

higher-order interactions) by comparing them with ‘classical’ dyadic network models (e.g. [7,8]). At the same time, model reconstruction of dyadic networks is sometimes known to paradoxically yield group interactions, e.g. in experiments with electrochemical oscillators [9]. Higher-order interaction networks have consequently found their way into various recent mathematical studies as well. We mention in particular the theoretical papers [10–16], which investigate synchronization in classes of networks with non-pairwise, nonlinear interactions in their equations of motion. We also refer to the excellent surveys [17–21] and references therein, for an in-depth discussion of higher-order networks, and numerous examples of higher-order network systems arising in applications.

This article builds on previous work of the authors [16], in which we generalized the notion of a *coupled cell network*, introduced by Golubitsky *et al.*, Golubitsky & Stewart and Field [22–24], to the context of higher-order networks. We did this by introducing a class of ‘hypernetworks’ and defining their ‘admissible’ maps and ordinary differential equations (ODEs), thus formalizing the notion of a dynamical system on a higher-order interaction network. We also introduced balanced colourings [22] of hypernetworks, and hypergraph fibrations [25,26], and used these concepts to classify the *robust synchrony patterns*, that is the synchrony spaces that are invariant under every admissible map, to hypernetwork dynamical systems.

The most surprising result in von der Gracht *et al.* [16] is the observation that the robust synchrony spaces of a hypernetwork system are not determined by linear terms in its equations of motion. This distinguishes hypernetworks from classical (dyadic) coupled cell networks, for which it was proved in Golubitsky *et al.* [27] that a synchrony space is invariant under every admissible map, if and only if it is invariant under every linear admissible map, see also [28]. On the contrary, we prove in von der Gracht *et al.* [16] that a synchrony space of a hypernetwork system is robustly invariant, whenever it is invariant under all polynomial admissible maps of a specific degree, which depends on the order of the hyperedges in the hypernetwork. Examples moreover show that our estimate for this polynomial degree is sharp.

As a consequence, a hypernetwork-admissible map of sufficiently low polynomial degree may admit ‘ghost’ synchrony spaces that are not supported by general, e.g. higher degree polynomial admissible maps. These ghost synchrony spaces may have a profound effect on the dynamics of the hypernetwork system. In particular, the final section of von der Gracht *et al.* [16] presents numerical evidence that they can give rise to a remarkable new type of local synchrony breaking bifurcation. The aim of this paper is to explain when and why such bifurcations occur.

We in fact observed this type of bifurcation in a one-parameter family of admissible ODEs for the hypernetwork depicted in figure 1a, meaning that these ODEs are of the form given in equation (2.3) below. Figure 1b displays two numerically obtained branches of steady states that emerge in a bifurcation in a particular system of this form. The steady-state branches were found by forward integrating the equations of motion—so they are asymptotically stable. We see that  $y_0 = y_1$  for negative values of the bifurcation parameter  $\lambda$ , so on the negative branch  $y_0$  and  $y_1$  are synchronous. On the positive branch,  $y_0$  and  $y_1$  are non-synchronous, i.e. for positive values of  $\lambda$  it holds that  $y_0 \neq y_1$ . However, even though  $y_0$  and  $y_1$  grow notably as  $\lambda$  increases, the difference  $y_0 - y_1$  only increases very slowly as a function of  $\lambda$ , and hence it appears that the branch is tangent to the synchrony space  $\{y_0 = y_1\}$ . In von der Gracht *et al.* [16], we called this phenomenon ‘reluctant synchrony breaking’. The term ‘reluctant’ is to be understood literally, and refers to the slow separation of the states of two nodes that were synchronous before the bifurcation. Importantly, the reluctance is not caused by any (external) physical influence. On the contrary, it is solely due to the topology of the interaction structure of the hypernetwork, as we show below. A more detailed numerical analysis, see figure 2a,b, suggests that  $y_0 - y_1 \sim \lambda^3$ , i.e. that the branch has a third order tangency to the synchrony space. In §4, we prove that this is indeed the case.

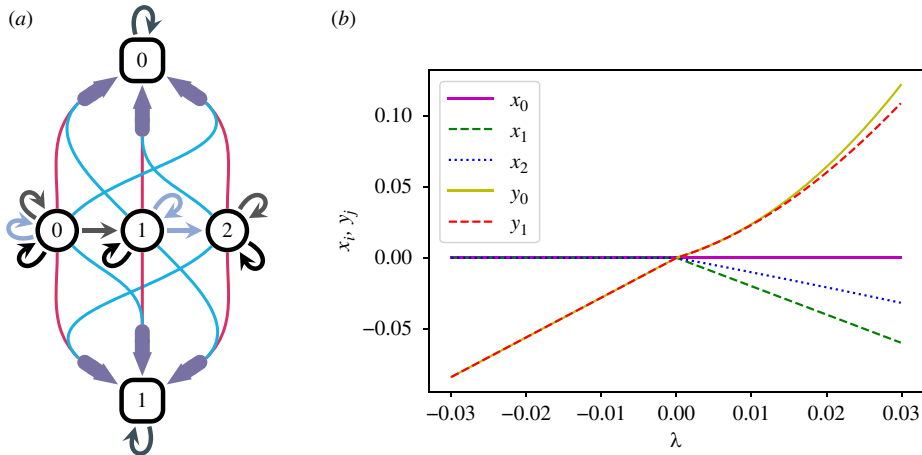


**Figure 1.** A hypernetwork that supports an unusual 'reluctant' synchrony breaking local steady-state branch. The round nodes in figure 1a correspond to the  $x$ -variables in (2.1), and the square nodes to the  $y$ -variables. The numerically obtained bifurcation branch in figure 1b satisfies  $y_0 = y_1$  for  $\lambda < 0$  and  $y_0 \neq y_1$  for  $\lambda > 0$ . We will prove in this paper that  $y_0 - y_1 \sim \lambda^3$  for  $\lambda > 0$ . (a) The hypernetwork that realizes the ODE system (2.1). (b) Numerically obtained bifurcation diagram for equations of the form (2.1). Figure taken from von der Gracht *et al.* [16].

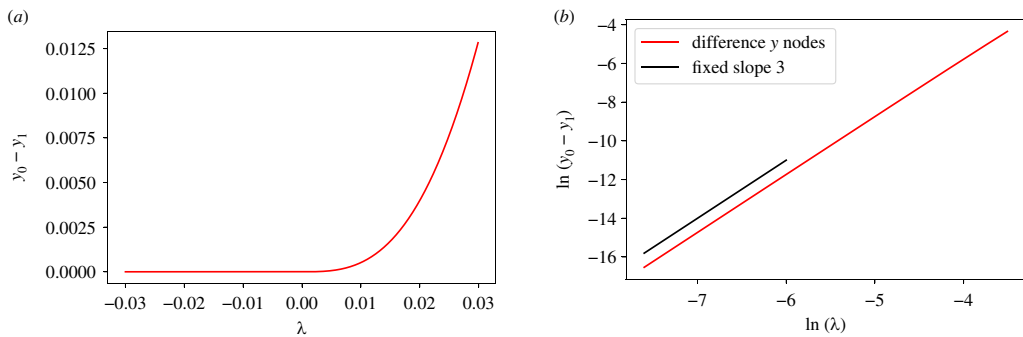


**Figure 2.** More details for the steady-state branches depicted in figure 1b. Figures taken from von der Gracht *et al.* [16]. (a) The difference between the  $y$ -nodes along the steady state branches. (b) A log–log plot of the difference between the  $y$ -nodes, for  $\lambda > 0$ . The black line segment in the log–log plot has slope 3 and was added to show that  $y_0(\lambda) - y_1(\lambda) \sim \lambda^3$ .

We show in this article that reluctant synchrony breaking is ubiquitous in hypernetworks. The main result that we present is theorem 4.2, which states that reluctant synchrony breaking occurs generically in one-parameter bifurcations in a large class of hypernetworks. These so-called augmented hypernetworks are constructed by coupling new nodes to an existing network or hypernetwork by means of specific higher-order interactions. The hypernetwork depicted in figure 1a is just one example of such an augmented hypernetwork. This means that the anomalous bifurcation that was discovered in von der Gracht *et al.* [16] and described above is not a numerical artefact. Instead, reluctant synchrony breaking is a generic phenomenon in ODEs of the form (2.3). To illustrate our main result, we present several more examples in this paper. We also argue (see remark 6) that one may design augmented hypernetworks that admit reluctant synchrony breaking bifurcation branches with an arbitrarily high order of reluctancy, i.e. an arbitrarily high order of tangency to a synchrony space.

*Structure of the article.* In §2, we illustrate reluctant synchrony breaking by studying the example presented in [16] in more detail. In §3, we summarize the theoretical findings of von

der Gracht *et al.* [16], in which we defined a class of dynamical systems on hypernetworks, studied their robust synchrony and balanced partitions, and introduced the so-called augmented hypernetwork. In §4, we prove our main result, theorem 4.2, which states that reluctant synchrony breaking occurs generically in augmented hypernetworks, and which provides a formula for the order of reluctancy of the synchrony breaking steady-state branch. We also apply the theorem to the example discussed in this introduction. In §5, the main theorem is illustrated by three more examples. A discussion of our results is presented in §6.

## 2. A first example

We now provide more details on the example that was briefly discussed in §1, and that was introduced and studied numerically in von der Gracht *et al.* [16]. As mentioned above, this example concerns the hypernetwork shown in figure 1a. In von der Gracht *et al.* [16], we introduced the class of *admissible ODEs* of a hypernetwork (see also §3). The admissible ODEs associated to the hypernetwork in figure 1a are all the ODEs of the form:

$$\begin{aligned}\dot{x}_0 &= G(x_0, x_0, x_0), \\ \dot{x}_1 &= G(x_1, x_1, x_0), \\ \dot{x}_2 &= G(x_2, x_1, x_2), \\ \dot{y}_0 &= F(y_0, (x_0, x_1), (x_1, x_2), (x_2, x_0)), \\ \dot{y}_1 &= F(y_1, (x_0, x_2), (x_1, x_0), (x_2, x_1)),\end{aligned}\tag{2.1}$$

for certain smooth functions  $F$  and  $G$ . We assume for now that the variables  $x_i, y_j$  take values in  $\mathbb{R}$ , so that  $F: \mathbb{R} \times \mathbb{R}^2 \times \mathbb{R}^2 \times \mathbb{R}^2 \rightarrow \mathbb{R}$  and  $G: \mathbb{R} \times \mathbb{R} \times \mathbb{R} \rightarrow \mathbb{R}$ . The brackets in  $F$  serve to distinguish the two-dimensional inputs from hyperedges of order two (the purple arrows in figure 1a). The assumption that these hyperedges are identical, translates into the requirement that  $F$  is invariant under all permutations of these pairs of variables. That is, we require that for all  $Y, X_1, \dots, X_6 \in \mathbb{R}$ ,

$$\begin{aligned}F(Y, (X_0, X_1), (X_2, X_3), (X_4, X_5)) &= \\ F(Y, (X_2, X_3), (X_0, X_1), (X_4, X_5)) &= \\ F(Y, (X_0, X_1), (X_4, X_5), (X_2, X_3)) &.\end{aligned}\tag{2.2}$$

To study bifurcations within this class of admissible ODEs, we parameterize the response functions  $F$  and  $G$  in (2.1) by a scalar variable  $\lambda$  taking values in some open neighbourhood  $\Omega \subseteq \mathbb{R}$  of the origin. This gives the one-parameter family of hypernetwork admissible ODEs:

$$\begin{aligned}\dot{x}_0 &= G(x_0, x_0, x_0; \lambda), \\ \dot{x}_1 &= G(x_1, x_1, x_0; \lambda), \\ \dot{x}_2 &= G(x_2, x_1, x_2; \lambda), \\ \dot{y}_0 &= F(y_0, (x_0, x_1), (x_1, x_2), (x_2, x_0); \lambda), \\ \dot{y}_1 &= F(y_1, (x_0, x_2), (x_1, x_0), (x_2, x_1); \lambda).\end{aligned}\tag{2.3}$$

To guarantee that the system (2.3) is admissible for every fixed value of  $\lambda \in \Omega$ , we assume  $F$  satisfies equation (2.2) for any fixed value of  $\lambda$ . Let us in addition assume:

$$F(0, (0, 0), (0, 0), (0, 0); 0) = G(0, 0, 0; 0) = 0,$$

so that the system (2.3) has a steady-state point at the origin for  $\lambda = 0$ . We may study the persistence of this steady-state by investigating the Jacobian at the origin of the system for  $\lambda = 0$ . To this end, we write:

$$F(Y, (X_0, X_1), (X_2, X_3), (X_4, X_5); \lambda) = aY + bX_0 + cX_1 + bX_2 + cX_3 + bX_4 + cX_5 + d\lambda + \mathcal{O}(\|(Y, X_0, \dots, X_5; \lambda)\|^2), \quad (2.4)$$

and

$$G(X_0, X_1, X_2; \lambda) = AX_0 + BX_1 + CX_2 + \mathcal{O}(\|\lambda\| + \|(X_0, X_1, X_2)\|^2), \quad (2.5)$$

with  $a, \dots, d, A, B, C \in \mathbb{R}$ , to specify the linear terms. The multiple occurrence of the terms  $b$  and  $c$  in (2.4) is due to the fact that according to (2.2),  $F$  depends in the same way on the tuple  $(X_0, X_1)$  as it does on  $(X_2, X_3)$  and  $(X_4, X_5)$ . In terms of these coefficients, the Jacobian matrix of the right-hand side of equation (2.3) at  $(x; \lambda) = (0, 0)$  with respect to the spatial variables  $x = (x_0, x_1, x_2, y_0, y_1)$  is:

$$\begin{pmatrix} A+B+C & 0 & 0 & 0 & 0 \\ C & A+B & 0 & 0 & 0 \\ 0 & B & A+C & 0 & 0 \\ b+c & b+c & b+c & a & 0 \\ b+c & b+c & b+c & 0 & a \end{pmatrix}.$$

The eigenvalues of this Jacobian are  $A+B+C$ ,  $A+B$  and  $A+C$  (all with multiplicity 1), and  $a$  (with algebraic and geometric multiplicity 2). To allow for a steady-state bifurcation to occur at  $\lambda=0$ , we consider the case  $A+B=0$ . We moreover assume the generic conditions  $a, A+B+C, A+C \neq 0$  to hold.

We claim that as  $\lambda$  is varied near 0, two branches of steady states will generically emerge from the origin. These can be found by first focusing on the subnetwork given by the three nodes of the same type. That is, we first solve

$$\begin{aligned} G(x_0, x_0, x_0; \lambda) &= 0, \\ G(x_1, x_1, x_0; \lambda) &= 0, \\ G(x_2, x_1, x_2; \lambda) &= 0. \end{aligned}$$

A direct calculation shows that, for generic values of the first- and second-degree Taylor coefficients of  $G$ , one of the steady-state branches is locally given by

$$x_0(\lambda) = x_1(\lambda) = x_2(\lambda) = x(\lambda) = D_0\lambda + \mathcal{O}(\|\lambda\|^2), \quad (2.6)$$

while another branch is given by:

$$x_0(\lambda) = D_0\lambda + \mathcal{O}(\|\lambda\|^2), \quad x_1(\lambda) = D_1\lambda + \mathcal{O}(\|\lambda\|^2), \quad x_2(\lambda) = D_2\lambda + \mathcal{O}(\|\lambda\|^2), \quad (2.7)$$

for certain non-zero and mutually distinct  $D_0, D_1, D_2 \in \mathbb{R}$ . For our choices of parameters, no further branches exist. We omit the computation of these branches. For a detailed exposition on how to compute steady-state bifurcation branches in so-called *feedforward networks* (i.e. networks with no loops other than self-loops), we refer to von der Gracht *et al.* [29].

We now turn to computing the values of  $y_0$  and  $y_1$  along the bifurcation branches. We start by looking at the first branch, given by equation (2.6). Restricted to this branch, the steady-state equation  $\dot{y}_0 = 0$  becomes:

$$F(y_0, (x(\lambda), x(\lambda)), (x(\lambda), x(\lambda)), (x(\lambda), x(\lambda)); \lambda) = 0. \quad (2.8)$$

Combining (2.4) and (2.6) this can be expanded as:

$$ay_0 + (3D_0(b+c) + d)\lambda + \mathcal{O}(\|(y_0; \lambda)\|^2) = 0,$$

which by the implicit function theorem has a unique solution given by:

$$y_0(\lambda) = \frac{-3D_0(b+c)-d}{a}\lambda + \mathcal{O}(|\lambda|^2).$$

Setting  $\dot{y}_1 = 0$  gives precisely the same equation to solve as (2.8), but with  $y_0$  replaced by  $y_1$ . Hence, we find  $y_0(\lambda) = y_1(\lambda)$  along this first branch, which we will therefore refer to as the *synchronous branch* of system (2.3).

We now turn to the second branch of steady states, of which the asymptotics of the  $x$ -variables is given by equation (2.7). Combining (2.4) with (2.7), we find that  $\dot{y}_0 = 0$  is equivalent to

$$ay_0 + ((b+c)(D_0 + D_1 + D_2) + d)\lambda + \mathcal{O}(\|y_0; \lambda\|^2) = 0.$$

It follows again from the implicit function theorem that locally precisely one solution exists, given by:

$$y_0(\lambda) = \frac{-(b+c)(D_0 + D_1 + D_2) - d}{a}\lambda + \mathcal{O}(|\lambda|^2). \quad (2.9)$$

In exactly the same way, we find that  $\dot{y}_1 = 0$  is solved for by

$$y_1(\lambda) = \frac{-(b+c)(D_0 + D_1 + D_2) - d}{a}\lambda + \mathcal{O}(|\lambda|^2). \quad (2.10)$$

Note that these expressions for  $y_0(\lambda)$  and  $y_1(\lambda)$  agree up to first order in  $\lambda$ . However, unlike for the synchronous branch, there is no reason to conclude that  $y_0(\lambda) = y_1(\lambda)$  along this branch, as the equations for  $\dot{y}_0$  and  $\dot{y}_1$  in (2.3) are different for distinct  $x_0, x_1$  and  $x_2$ :

$$\begin{aligned} F(y_0, (x_0(\lambda), x_1(\lambda)), (x_1(\lambda), x_2(\lambda)), (x_2(\lambda), x_0(\lambda)); \lambda) &= 0, \\ F(y_1, (x_0(\lambda), x_2(\lambda)), (x_1(\lambda), x_0(\lambda)), (x_2(\lambda), x_1(\lambda)); \lambda) &= 0. \end{aligned}$$

We will refer to the branch of steady states given by equations (2.7), (2.9) and (2.10) as the *reluctant branch* of (2.3).

Figure 1b demonstrates numerically that the reluctant branch is truly non-synchronous. The figure was taken from von der Gracht *et al.* [16], and it shows a numerically obtained plot of the asymptotically stable bifurcation branches that emerge in a bifurcation in a particular realization of system (2.3), namely for the choices

$$\begin{aligned} G(X_0, X_1, X_2; \lambda) &= -X_0 + X_1 - X_2 + 8\lambda X_0 + 4X_0^2 \text{ and} \\ F(Y, (X_0, X_1), (X_2, X_3), (X_4, X_5); \lambda) &= -5Y + 14\lambda \\ &\quad - h(10X_0 - 12X_1) - h(10X_2 - 12X_3) - h(10X_4 - 12X_5) \end{aligned}$$

in which,

$$h(x) = \sin(x) + \cos(x) - 1. \quad (2.11)$$

It is known from von der Gracht *et al.* [29] that for this choice of  $G$ , the steady-state branch  $x(\lambda)$  is stable inside the subnetwork given by the three nodes of the same type. The negative coefficient in front of the linear  $Y$ -term in  $F$  implies that it is stable in the  $y$ -directions as well—so that it can easily be found numerically. Figure 1b shows the synchronous branch for  $\lambda < 0$  and the reluctant branch for  $\lambda > 0$ —indeed,  $y_0$  and  $y_1$  agree for  $\lambda < 0$ , and quite clearly do not for  $\lambda > 0$ . This becomes even more visible in figure 2a, which shows  $y_0 - y_1$  as a function of  $\lambda$ . The logarithmic plot in figure 2b suggests that  $y_0(\lambda) - y_1(\lambda) \sim \lambda^3$ . In §4, we prove that this is truly the case.

In this article, we rigorously prove the existence of reluctant steady-state branches in bifurcations in a large class of hypernetwork systems. Specifically, we will show that reluctant bifurcation branches appear in generic one-parameter local synchrony breaking steady-state

bifurcations in the admissible ODEs for such hypernetworks. We also provide a formula for the order in  $\lambda$  with which the ‘reluctant nodes’ separate.

### 3. Preliminaries

In this section, we briefly introduce hypernetwork dynamical systems and summarize results obtained in von der Gracht *et al.* [16]. In fact, in von der Gracht *et al.* [16], we define a hypernetwork to be a collection  $\mathbf{N} = (V, H, s, t)$  consisting of a finite set of *vertices* or *nodes*  $V$ , a finite set of *hyperedges*  $H$  and source and target maps  $s$  and  $t$  defined on  $H$ . Given an edge  $h \in H$ , its target  $t(h) \in V$  is a single vertex, whereas the source  $s(h) = (s_1(h), \dots, s_{k_h}(h)) \in V^{k_h}$  is an ordered  $k_h$ -tuple of vertices. The number  $k_h > 0$  depends on the hyperedge  $h$ , and is called its *order*. To avoid cluttered notation though, we often suppress the dependence of  $k_h$  on  $h$  when it is clear from context, and simply write  $k$ . Note that the  $k_h$  vertices in  $s(h)$  are not required to be distinct. The order of a hypernetwork  $\mathbf{N}$  is then defined as the maximum of the orders of its hyperedges, so that the hypernetworks of order 1 are precisely the classical (dyadic) networks.

In addition to the data that are explicitly given in  $\mathbf{N} = (V, H, s, t)$ , we also specify equivalence relations on both the nodes  $V$  and the hyperedges  $H$ . We typically refer to both as the *colour* or *type* relation. The reason that these relations are not specified in  $\mathbf{N}$  is because they will apply to all hypernetworks at once. That is, it will make sense for two nodes in different hypernetworks to have the same colour, and likewise for multiple hyperedges across different hypernetworks. This allows us to define node- and hyperedge-type preserving maps between different hypernetworks, which in turn give rise to semi-conjugacies between the dynamics, see von der Gracht *et al.* [16] for more details. Intuitively, this colour-relation conveys whether two nodes correspond to comparable or incomparable agents in a real-world system modelled by the hypernetwork, and similarly whether or not two hyperedges specify the same influence. As is suggested by this interpretation, the vertex- and hyperedge-types have to satisfy certain consistency conditions. These are:

- (i) if two nodes  $v_0$  and  $v_1$  are of the same type, then there exists a hyperedge-type preserving bijection between the set of hyperedges targeting  $v_0$  and those targeting  $v_1$ ;
- (ii) two hyperedges  $h_0, h_1$  of the same type have the same order  $k$ , and for each  $i \in \{1, \dots, k\}$  the nodes  $s_i(h_0)$  and  $s_i(h_1)$  are of the same vertex-type.

These conditions allow us to define dynamical systems with the interaction structure of the given hypernetwork. Such dynamical systems are specified by so-called *admissible* vector fields. To introduce these, we fix an internal phase space  $\mathbb{R}^{n_v}$  for each node  $v \in V$ , which will be identical for nodes of the same type. Each node  $v$  is given a state variable  $x_v \in \mathbb{R}^{n_v}$ . The *total phase space* of the hypernetwork dynamical system describes the states of all these variables, and is thus the direct sum  $\bigoplus_{v \in V} \mathbb{R}^{n_v}$ . We also specify, for each hyperedge  $h \in H$ , the vector of its source variables:

$$\mathbf{x}_{s(h)} = (x_{s_1(h)}, \dots, x_{s_{k_h}(h)}) \in \bigoplus_{i=1}^{k_h} \mathbb{R}^{n_{s_i(h)}}.$$

Next, we choose for each node  $v \in V$  its *response function*

$$F_v: \bigoplus_{h: t(h)=v} \bigoplus_{i=1}^{k_h} \mathbb{R}^{n_{s_i(h)}} \rightarrow \mathbb{R}^{n_v}. \quad (3.1)$$

These functions must satisfy certain conditions that reflect our intuitive idea that hyperedges of the same type encode identical influence, as well as the notion that nodes of the same type

respond to their input in the same way. In words, we require that the variables of identical-type hyperedges may be freely interchanged in  $F_v$ , as well as that  $F_v$  and  $F_w$  are the same when the nodes  $v$  and  $w$  are of the same type, after an appropriate identification of their domains. We may capture both requirements in one succinct condition as follows: given nodes  $v$  and  $w$  of the same type, for any hyperedge-type preserving bijection  $\alpha : t^{-1}(v) \rightarrow t^{-1}(w)$  we have:

$$F_w \left( \bigoplus_{t(h_2)=w} \mathbf{x}_{s(h_2)} \right) = F_v \left( \bigoplus_{t(h_1)=v} \mathbf{x}_{s(\alpha(h_1))} \right), \quad (3.2)$$

for all  $x = \bigoplus_{v \in V} x_v \in \bigoplus_{v \in V} \mathbb{R}^{n_v}$ . Recall that at least one such  $\alpha$  exists when  $v$  and  $w$  are of the same type. Finally, we define the *hypernetwork admissible vector field*

$$f^{\mathbf{N}}: \bigoplus_{v \in V} \mathbb{R}^{n_v} \rightarrow \bigoplus_{v \in V} \mathbb{R}^{n_v},$$

on the total phase space, to be given component-wise by:

$$f_v^{\mathbf{N}}(x) = F_v \left( \bigoplus_{h: t(h)=v} \mathbf{x}_{s(h)} \right)$$

for all  $v \in V$  and  $x \in \bigoplus_{v \in V} \mathbb{R}^{n_v}$ .

To study synchronization in hypernetwork dynamical systems, we define a *polysynchrony subspace* to be a subspace of the total phase space of a hypernetwork that is determined by equality of clusters of node variables. More precisely, for any partition  $P = \{V_1, \dots, V_C\}$  of the nodes  $V$  of a hypernetwork, one can define the polysynchrony subspace

$$\text{Syn}_P = \{x_v = x_w \text{ when } v \text{ and } w \text{ are in the same element of } P\}.$$

Such a polysynchrony subspace is called *robust* if it is invariant under the flow of any admissible vector field, that is, when  $f^{\mathbf{N}}(\text{Syn}_P) \subseteq \text{Syn}_P$  for every admissible vector field  $f^{\mathbf{N}}$ . It was shown in von der Gracht *et al.* [16] that  $\text{Syn}_P$  is robust if and only if  $P$  is *balanced*, meaning that the partition is ‘consistent with the hypernetwork structure’. For the precise definition of a balanced partition, we refer to von der Gracht *et al.* [16]. It was also shown in von der Gracht *et al.* [16] that a partition  $P$  is balanced (and hence  $\text{Syn}_P$  is robust) if and only if  $\text{Syn}_P$  is invariant under all polynomial admissible vector fields of degree at most  $k(k+1)/2$ , where  $k$  is the order of the hypernetwork.

**Example 3.1.** One can show that the hypernetwork discussed in §2 and depicted in figure 1a has four robust synchrony subspaces (apart from the total phase space itself), namely  $\{x_0 = x_1\}$ ,  $\{x_0 = x_1 = x_2\}$ ,  $\{x_0 = x_1 \text{ and } y_0 = y_1\}$  and  $\{x_0 = x_1 = x_2 \text{ and } y_0 = y_1\}$ .

Of particular interest in this paper are so-called *augmented hypernetworks*, also introduced in von der Gracht *et al.* [16]. Their definition involves the symmetric group on  $k+1$  elements, denoted by  $S_{k+1}$ , which acts on the ordered set  $\{0, \dots, k\}$  by permutations. We denote by  $S_{k+1}^0$  and  $S_{k+1}^1$  the subsets of even and odd permutations, respectively, and denote by  $\text{sgn}(\sigma) \in \{0, 1\}$  the sign of a permutation  $\sigma \in S_{k+1}^{\text{sgn}(\sigma)}$ .

**Definition 3.2.** (Definition 5.1 in von der Gracht *et al.* [16].) Let  $\mathbf{N}$  be a hypernetwork with  $k+1 \geq 3$  nodes  $v_0, \dots, v_k$  of the same type. We define the *augmented hypernetwork with core*  $\mathbf{N}$ , denoted by  $\mathbf{N}^\diamond$ , as the hypernetwork obtained by adding two additional nodes  $w_0, w_1$ , one self-loop for each  $w_i$  and  $(k+1)!$  new hyperedges to  $\mathbf{N}$ . The new nodes are of the same type, which differs from that of the  $v_i$ . Likewise, we construct a new hyperedge-type that we assign to the  $(k+1)!$  additional hyperedges. Necessarily, the self-loops on the new nodes are of a same, new type too. The  $(k+1)!$  new hyperedges are indexed by the symmetric group  $S_{k+1}$ , so that we may denote them by  $h_\sigma$  for  $\sigma \in S_{k+1}$ . We define their sources and targets by

$$t(h_\sigma) = w_{\text{sgn}(\sigma)} \quad \text{and} \quad s(h_\sigma) = (v_{\sigma(1)}, \dots, v_{\sigma(k)}), \quad (3.3)$$

where  $S_{k+1}$  acts on the ordered set  $\{0, \dots, k\}$ . Note that  $v_{\sigma(0)} \in \{v_0, \dots, v_k\}$  is therefore the only  $v$ -node not in the source of  $h_\sigma$ , and that these hyperedges all have order  $k$ .

**Example 3.3.** The hypernetwork discussed in §2 and depicted in figure 1a is an example of an augmented hypernetwork. Here, the core consists of the  $k+1=3$  circular nodes in the centre and the arrows between them. The core in fact forms a classical (dyadic) network. The two ‘added’ nodes are depicted as the square ones. Equation (2.1) gives the form of a general admissible vector field for this augmented hypernetwork. Recall that the response function  $F$  in equation (2.1) is invariant under permutations of the three pairs of inputs, which reflects that the six ‘added’ hyperedges are all of the same type.

By assumption, all nodes in the core  $\mathbf{N}$  of an augmented hypernetwork are of the same type, so that  $\mathbf{N}^\diamond$  has precisely two node-types. This means that two response functions are required to describe an admissible vector field  $f^{\mathbf{N}^\diamond}$  for  $\mathbf{N}^\diamond$ . We will usually denote these by  $F$  and  $G$ , where  $G$  is used for the nodes in  $\mathbf{N}$  and  $F$  for the two additional nodes. Likewise, we see that the total phase space is determined by two vector spaces: one for the internal dynamics of the  $v$ -nodes,  $\mathbb{R}^{n_v}$ , and one for that of the  $w$ -nodes,  $\mathbb{R}^{n_w}$ . We will later set both equal to  $\mathbb{R}$ . Note that  $F$  takes one argument from  $\mathbb{R}^{n_w}$ , corresponding to the self-loop, and  $(k+1)!/2$  entries from  $\bigoplus^k \mathbb{R}^{n_v}$  for the remaining hyperedges. As these latter hyperedges are indexed by (half of) the symmetric group, we may see the response function as

$$F: \mathbb{R}^{n_w} \oplus \bigoplus_{\sigma \in S_{k+1}^0} \left( \bigoplus^k \mathbb{R}^{n_v} \right) \rightarrow \mathbb{R}^{n_w},$$

with the property that the  $(k+1)!/2$  entries with values in  $\bigoplus^k \mathbb{R}^{n_v}$  may be freely interchanged. Note that we simply index these entries by  $S_{k+1}^0$  to emphasize that they correspond to the hyperedges that are indexed by (part of) the symmetric group. We could have also used  $S_{k+1}^1$  and, because we may freely interchange these entries, we do not have to give an explicit identification between  $S_{k+1}^0$  and  $S_{k+1}^1$ . In particular, in any augmented hypernetwork the dynamics of the  $w$ -nodes may simply be written as

$$\dot{y}_0 = F \left( y_0, \bigoplus_{\sigma \in S_{k+1}^0} \mathbf{x}_\sigma \right) \quad \text{and} \quad \dot{y}_1 = F \left( y_1, \bigoplus_{\sigma \in S_{k+1}^1} \mathbf{x}_\sigma \right), \quad (3.4)$$

where  $\mathbf{x}_\sigma = (x_{\sigma(1)}, \dots, x_{\sigma(k)})$ , and where we write  $y_i$  for the state of node  $w_i$  and  $x_j$  for the state of node  $v_j$ .

**Remark 1.** We may generalize the definition of an augmented hypernetwork by connecting the auxiliary nodes  $w_0$  and  $w_1$  only to a subset  $\mathcal{S}$  of nodes of the same type of the core, consisting of  $k+1$  nodes of the same type. In this case, the nodes in the core that are not elements of  $\mathcal{S}$  may in fact be of different type. We can then add  $(k+1)!$  hyperedges of order  $k$ , precisely as in definition 3.2, but now with all source nodes in  $\mathcal{S}$ . It will be clear that our results also hold for such hypernetworks, but to avoid a cluttered exposition we will mostly work with definition 3.2. See also remark 5.

## 4. Reluctant synchrony-breaking

We now show that the reluctant synchrony breaking observed in §2 is not a peculiarity of systems of the form (2.3), but can occur in any augmented hypernetwork. In fact, we shall give natural conditions on the core  $\mathbf{N}$  that guarantee that reluctant synchrony breaking occurs

generically in the augmented hypernetwork  $\mathbf{N}^\diamond$ . Moreover, in theorem 4.2 below, we give a precise expression for the degree (in the bifurcation parameter) at which the reluctant synchrony breaking occurs. We start by introducing some useful notation and conventions.

As it is sometimes convenient to make explicit the dependence of an admissible vector field on its response functions, we will often write  $f_{(F,G)}^{\mathbf{N}^\diamond}$  and  $f_{(G)}^{\mathbf{N}}$  for the admissible vector fields of  $\mathbf{N}^\diamond$  and  $\mathbf{N}$ , respectively. Furthermore, because in this section we are mainly interested in bifurcations, we will often use  $f^{\mathbf{N}}$  (and  $f^{\mathbf{N}^\diamond}$ ,  $f_{(F,G)}^{\mathbf{N}^\diamond}$ , etc.) to denote parameter families of admissible vector fields. This means  $f^{\mathbf{N}}$  is an admissible vector field for any fixed value of the bifurcation parameter, as in §2.

Throughout this section, we will investigate asymptotics and power series in  $\lambda$  for bifurcation branches. Some of these might involve fractional powers of  $\lambda$ , meaning that such branches are only defined for positive or negative values of  $\lambda$ . To keep this section as readable as possible, we assume from here on out that all branches are defined for positive values of  $\lambda$ , so that we may always write  $\lambda^p$  for any power  $p \geq 0$ . The corresponding results for negative values of  $\lambda$  follow easily by redefining  $\lambda$  as  $-\lambda$ . For a function  $X = X(\lambda)$  defined for small positive values of  $\lambda$ , we will frequently use the abbreviation  $X(\lambda) \sim \lambda^p$  to denote that there exists a constant  $A \neq 0$  for which  $X(\lambda) = A\lambda^p + \text{'higher order terms in } \lambda\text{'}$ .

**Definition 4.1.** Let  $\mathbf{N}$  be a hypernetwork with  $n$  nodes and denote by  $f^{\mathbf{N}}: \mathbb{R}^n \times \Omega \rightarrow \mathbb{R}^n$  a one-parameter family of admissible vector fields for  $\mathbf{N}$ , where each node has a one-dimensional internal phase space. In this paper, a locally defined branch of steady states  $x(\lambda) = (x_1(\lambda), \dots, x_n(\lambda))$  for  $f^{\mathbf{N}}$  is called *fully synchrony-breaking* if for all  $i, j \in \{1, \dots, n\}$  with  $i > j$  there exist numbers  $p_{i,j} > 0$  such that:

$$x_i(\lambda) - x_j(\lambda) \sim \lambda^{p_{i,j}}. \quad (4.1)$$

Given a fully synchrony-breaking steady-state branch, we define its *order of asynchrony* as the number:

$$\bar{p} = \sum_{\substack{i,j=1 \\ i>j}}^n p_{i,j}. \quad (4.2)$$

In what follows, we will need to make some assumptions about the asymptotics and regularity of the branches. To avoid a detailed exposition, we instead use a formal ansatz. From here on out, we will always assume a fully synchrony-breaking branch  $x(\lambda) = (x_1(\lambda), \dots, x_n(\lambda))$  to come with a finite set of numbers  $\Upsilon \subseteq (0, \bar{p}]$  such that we may write:

$$x_i(\lambda) = \sum_{p \in \Upsilon} A_{i,p} \lambda^p + \mathcal{O}(|\lambda|^{\bar{p}+\epsilon}) \quad (4.3)$$

for some  $\epsilon > 0$ , and with  $A_{i,p} \in \mathbb{R}$ . Note that these  $A_{i,p}$  may very well vanish. As we may write:

$$\begin{aligned} x_i(\lambda) - x_j(\lambda) &= \sum_{p \in \Upsilon} (A_{i,p} - A_{j,p}) \lambda^p + \mathcal{O}(|\lambda|^{\bar{p}+\epsilon}) \\ &= D_{i,j} \lambda^{p_{i,j}} + \text{'higher-order terms'}, \end{aligned} \quad (4.4)$$

and because  $p_{i,j} \leq \bar{p}$ , we see that necessarily  $p_{i,j} \in \Upsilon$  for all  $i > j$ . Note that the  $D_{i,j}$  appearing in (4.4) are all non-zero by assumption (4.1).

Equation (4.4) also shows that  $A_{i,p_{i,j}}$  and  $A_{j,p_{i,j}}$  cannot both be 0, as this would imply  $D_{i,j} = 0$ . As a result, we see that at least one of the components  $x_i(\lambda)$  and  $x_j(\lambda)$  grows as  $\lambda^s$  with  $s \leq p_{i,j}$ . Given  $k \in \{1, \dots, n\}$  let us denote by  $s_k$  the order of  $x_k(\lambda)$ , so that  $x_k(\lambda) \sim \lambda^{s_k}$ . If  $x_k(\lambda) = 0$  then we may set  $s_k = \infty$ . What we have argued is simply that  $\min(s_i, s_j) \leq p_{i,j}$ .

A related quantity appearing in theorem 4.2 below will be

$$\hat{p} = \min(s_1, \dots, s_n, 1). \tag{4.5}$$

It follows that:

$$\hat{p} \leq \min(s_1, s_2) \leq p_{1,2} < \bar{p}, \tag{4.6}$$

as  $p_{i,j} > 0$  for all  $i, j$ .

In the theorem below, we assume all admissible vector fields correspond to one-dimensional internal dynamics for each node.

**Theorem 4.2.** *Let  $\mathbf{N}^\diamond$  be an augmented hypernetwork with core  $\mathbf{N}$ , the latter consisting of  $k + 1 \geq 3$  nodes, and let  $f_{(G)}^{\mathbf{N}}: \mathbb{R}^{k+1} \times \Omega \rightarrow \mathbb{R}^{k+1}$  be a one-parameter family of admissible vector fields for  $\mathbf{N}$ , corresponding to some response function  $G$ . Assume  $f_{(G)}^{\mathbf{N}}$  admits a fully synchrony-breaking branch of steady states  $x(\lambda) = (x_0(\lambda), \dots, x_k(\lambda))$  with order of asynchrony  $\bar{p}$ .*

*Then for a generic  $\lambda$ -dependent response function  $F = F(\cdot; \lambda)$ , the system  $f_{(F,G)}^{\mathbf{N}^\diamond}: \mathbb{R}^{k+3} \times \Omega \rightarrow \mathbb{R}^{k+3}$  admits a steady-state branch  $z(\lambda) = (x_0(\lambda), \dots, x_k(\lambda), y_0(\lambda), y_1(\lambda))$  for which:*

$$y_0(\lambda), y_1(\lambda) \sim \lambda^{\hat{p}} \text{ while } y_0(\lambda) - y_1(\lambda) \sim \lambda^{\bar{p}}.$$

The branch  $z(\lambda)$  consists of asymptotically stable equilibria for  $f_{(F,G)}^{\mathbf{N}^\diamond}$  if and only if  $x(\lambda)$  consists of asymptotically stable equilibria for  $f_{(G)}^{\mathbf{N}}$  and  $\partial F / \partial y(0; 0) < 0$ .

Note that, since  $\hat{p} < \bar{p}$  by equation (4.6), we see that the branch found in theorem 4.2 is truly tangent to the space  $\{y_0 = y_1\}$ . In other words, the difference between the  $y$ -components grows significantly slower than the two  $y$ -values themselves.

**Remark 2.** As  $(f_{(-F,G)}^{\mathbf{N}^\diamond})_w = -(f_{(F,G)}^{\mathbf{N}^\diamond})_w$  for the two nodes  $w$  outside the core, we see that  $z(\lambda)$  is a branch of steady-states for  $f_{(F,G)}^{\mathbf{N}^\diamond}$ , if and only if it is for  $f_{(-F,G)}^{\mathbf{N}^\diamond}$ . The stability condition in theorem 4.2 holds for either  $f_{(F,G)}^{\mathbf{N}^\diamond}$  or  $f_{(-F,G)}^{\mathbf{N}^\diamond}$ . Hence, each existing branch that is stable for the core is stable for either  $f_{(F,G)}^{\mathbf{N}^\diamond}$  or for  $f_{(-F,G)}^{\mathbf{N}^\diamond}$ . This can be particularly useful if one wants to realize all branches (not just the stable ones) numerically.

Before proving the theorem, we first apply it to our running example.

**Example 4.3.** In §2, we investigated a bifurcation scenario with a fully synchrony-breaking branch in the core, given by  $x_i(\lambda) = D_i \lambda + \mathcal{O}(|\lambda|^2)$  for  $i \in \{0,1,2\}$  and with mutually distinct  $D_i$ . It follows that  $x_i(\lambda) - x_j(\lambda) = (D_i - D_j)\lambda + \mathcal{O}(|\lambda|^2)$  for all  $i, j$ . As  $D_i - D_j \neq 0$  for  $i > j$ , we obtain  $p_{3,1} = p_{3,2} = p_{2,1} = 1$  and hence

$$\bar{p} = 1 + 1 + 1 = 3.$$

Theorem 4.2 therefore predicts a bifurcation branch  $z(\lambda) = (x_0(\lambda), x_1(\lambda), x_2(\lambda), y_0(\lambda), y_1(\lambda))$  in the augmented system  $f_{(F,G)}^{\mathbf{N}^\diamond}$  for a generic choice of  $F$  and with any  $G$  supporting the aforementioned fully synchrony-breaking branch in the core, which satisfies:

$$y_0(\lambda) - y_1(\lambda) \sim \lambda^3.$$

This is indeed what we found in our numerical investigation, see figure 2b.

The proof of theorem 4.2 requires some machinery from von der Gracht *et al.* [16]. There we introduced the polynomials  $P_{(k)}: \bigoplus_{\sigma \in S_{k+1}^0} \mathbb{R}^k \rightarrow \mathbb{R}$ , given by:

$$P_{(k)} \left( \bigoplus_{\sigma \in S_{k+1}^0} \mathbf{X}_\sigma \right) = \sum_{\sigma \in S_{k+1}^k} X_{\sigma,1}^1 X_{\sigma,2}^2 \cdots X_{\sigma,k}^k, \tag{4.7}$$

for  $k \in \mathbb{N}$ , and where  $\mathbf{X}_\sigma = (X_{\sigma,1}, \dots, X_{\sigma,k}) \in \mathbb{R}^k$  for  $\sigma \in S_{k+1}^0$ . We also state the following result, a proof of which can be found in von der Gracht *et al.* [16].

**Lemma 4.4.** (Lemma 5.6 in von der Gracht *et al.* [16].) *Let  $Q: \bigoplus_{\sigma \in S_{k+1}^0} \mathbb{R}^k \rightarrow \mathbb{R}$  be a polynomial function that is invariant under all permutations of its  $\#S_{k+1}^0$  entries from  $\mathbb{R}^k$ . Then there exists a polynomial  $S: \mathbb{R}^{k+1} \rightarrow \mathbb{R}$  such that:*

$$Q\left(\bigoplus_{\sigma \in S_{k+1}^0} \mathbf{x}_\sigma\right) - Q\left(\bigoplus_{\sigma \in S_{k+1}^1} \mathbf{x}_\sigma\right) = S(x) \prod_{\substack{i,j=0 \\ i>j}}^k (x_i - x_j) \tag{4.8}$$

for all  $x = (x_0, \dots, x_k) \in \mathbb{R}^{k+1}$ , where  $\mathbf{x}_\sigma = (x_{\sigma(1)}, \dots, x_{\sigma(k)})$  for all  $\sigma \in S_{k+1}$ .

**Remark 3.** It can readily be seen that for any polynomial  $Q$  satisfying the conditions of lemma 4.4, (4.8) is actually equivalent to the fact that

$$Q\left(\bigoplus_{\sigma \in S_{k+1}^0} \mathbf{x}_\sigma\right) = Q\left(\bigoplus_{\sigma \in S_{k+1}^1} \mathbf{x}_\sigma\right), \tag{4.9}$$

whenever  $(x_0, \dots, x_k) \in \mathbb{R}^{k+1}$  satisfies  $x_i = x_j$  for some distinct  $i, j \in \{0, \dots, k\}$ . This observation still holds when  $Q$  is not polynomial, see lemma 5.5 of von der Gracht *et al.* [16]. The latter fact actually underlies the proof of lemma 4.4 that is given in [16].

**Lemma 4.5.** *The polynomials  $P_{(k)}$  defined in (4.7) satisfy:*

$$P_{(k)}\left(\bigoplus_{\sigma \in S_{k+1}^0} \mathbf{x}_\sigma\right) - P_{(k)}\left(\bigoplus_{\sigma \in S_{k+1}^1} \mathbf{x}_\sigma\right) = \prod_{\substack{i,j=0 \\ i>j}}^k (x_i - x_j), \tag{4.10}$$

for all  $x = (x_0, \dots, x_k) \in \mathbb{R}^{k+1}$ .

*Proof.* By lemma 4.4, we have:

$$P_{(k)}\left(\bigoplus_{\sigma \in S_{k+1}^0} \mathbf{x}_\sigma\right) - P_{(k)}\left(\bigoplus_{\sigma \in S_{k+1}^1} \mathbf{x}_\sigma\right) = S(x) \prod_{\substack{i,j=0 \\ i>j}}^k (x_i - x_j),$$

for some polynomial  $S$ . It remains to show that  $S = 1$ . To this end, note that both the left- and right-hand side of equation (4.10) has total degree  $1 + \dots + k = k(k+1)/2$ . This means  $S$  is a constant polynomial. As both sides of equation (4.10) contain a term  $1 \cdot x_1 x_2^2 \dots x_k^k$ , we see that  $S = 1$  and the result follows.

Before we move on to the proof of theorem 4.2, we first have a closer look at the set of powers  $\Upsilon$ . Recall that we may write:

$$x_i(\lambda) = \sum_{p \in \Upsilon} A_{i,p} \lambda^p + \mathcal{O}(|\lambda|^{p+\epsilon}), \tag{4.11}$$

for all the components  $x_i(\lambda)$  of a fully synchrony-breaking branch. By adding zero-coefficients  $A_{i,p}$  to expression (4.11) and by decreasing  $\epsilon$  if needed, we may assume that for all  $p, q \in \Upsilon$ , we have:

$$\begin{aligned} p+q \in \Upsilon & \text{ if } p+q \leq \bar{p}; \\ p+q \geq \bar{p}+\epsilon & \text{ if } p+q > \bar{p}, \end{aligned} \tag{4.12}$$

and also that:

$$\begin{aligned} 1 \in \Upsilon & \text{ if } 1 \leq \bar{p}; \\ 1 \geq \bar{p}+\epsilon & \text{ if } 1 > \bar{p}. \end{aligned}$$

More precisely, we can add to  $\Upsilon$  all non-zero sums  $s = c + \sum_{p \in \Upsilon} c_p p$  with non-negative integer coefficients  $c, c_p$ , such that  $s \leq \bar{p}$ . Note that this adds a finite number of elements to  $\Upsilon$ ,

as necessarily  $c_p \leq \lceil \bar{p}/p \rceil$  and  $c \leq \lceil \bar{p} \rceil$ . It then follows from equation (4.12) that  $\bar{p} \in \Upsilon$ , as we have  $p_{i,j} \in \Upsilon$  for all  $i > j$ . This allows us to iteratively investigate coefficients corresponding to (possibly non-integer) powers of  $\lambda$  in the branches, as well as in polynomial expressions involving the components of these branches. For instance, if  $x_1(\lambda)$  and  $x_2(\lambda)$  are given by equation (4.11), then we may likewise write:

$$\begin{aligned} x_1(\lambda)x_2(\lambda) &= \sum_{p \in \Upsilon} A'_p \lambda^p + \mathcal{O}(|\lambda|^{\bar{p}+\epsilon}) \text{ and} \\ \lambda x_1(\lambda) &= \sum_{p \in \Upsilon} A''_p \lambda^p + \mathcal{O}(|\lambda|^{\bar{p}+\epsilon}) \end{aligned}$$

for some  $A'_p, A''_p \in \mathbb{R}$ . Finally, whenever

$$w(\lambda) = \sum_{p \in \Upsilon} A_p \lambda^p + \mathcal{O}(|\lambda|^{\bar{p}+\epsilon}),$$

for some locally defined map  $w: \mathbb{R}_{\geq 0} \mapsto \mathbb{R}$  and with  $A_p \in \mathbb{R}$ , then for  $q \in \Upsilon$  we may write:

$$[w(\lambda)]_{\leq q} := \sum_{\substack{p \in \Upsilon \\ p \leq q}} A_p \lambda^p \text{ and } [w(\lambda)]_{< q} := \sum_{\substack{p \in \Upsilon \\ p < q}} A_p \lambda^p,$$

for the truncated power series.

*Proof of theorem 4.2.* By assumption,  $x(\lambda) = (x_0(\lambda), \dots, x_k(\lambda))$  locally solves  $(f_{(F,G)}^{\mathbf{N}^\circ}(x, y; \lambda))_v = (f_{(G)}^{\mathbf{N}}(x; \lambda))_v = 0$  for all nodes  $v$  in the core  $\mathbf{N}$  and all  $y = (y_0, y_1) \in \mathbb{R}^2$ . To solve for the  $y$ -components, let  $K \in \mathbb{N}$  be such that:

$$(K+1) \min(p \mid p \in \Upsilon) > \bar{p}. \quad (4.13)$$

We expand a general response function  $F$  as:

$$F(Y, \mathbf{X}; \lambda) = aY + \sum_{\ell, m=0}^K Q_{\ell, m}(\mathbf{X}) Y^\ell \lambda^m + \mathcal{O}(\|\mathbf{X}, Y; \lambda\|^{K+1}), \quad (4.14)$$

for  $Y \in \mathbb{R}$ ,  $\lambda \in \mathbb{R}_{\geq 0}$ , and where

$$\mathbf{X} := \bigoplus_{\sigma \in S_{k+1}^0} \mathbf{X}_\sigma,$$

with  $\mathbf{X}_\sigma \in \mathbb{R}^k$ . Here each  $Q_{\ell, m}$  is a polynomial of degree at most  $K$  that is invariant under all permutations of the vectors  $\mathbf{X}_\sigma$ , which follows from the fact that  $F$  is invariant under permutations of these vectors. Our assumption (which is necessary for a bifurcation) that  $F(0,0;0) = 0$  implies that  $Q_{0,0}(0) = 0$ . Moreover, by setting the number  $a \in \mathbb{R}$  equal to the derivative of  $F$  at  $(0,0;0)$  in the  $Y$ -direction, we may assume that  $Q_{1,0}(0) = 0$ .

For  $s \in \{0,1\}$ , the equation  $\dot{y}_s = 0$  gives:

$$ay_s + \sum_{\ell, m=0}^K Q_{\ell, m} \left( \bigoplus_{\sigma \in S_{k+1}^0} \mathbf{x}_\sigma(\lambda) \right) y_s^\ell \lambda^m + \mathcal{O}(\|(x(\lambda), y_s; \lambda)\|^{K+1}) = 0, \quad (4.15)$$

where  $\mathbf{x}_\sigma(\lambda) = (x_{\sigma(1)}(\lambda), \dots, x_{\sigma(k)}(\lambda))$  for all  $\sigma \in S_{k+1}$ . If we assume  $a \neq 0$  then by the implicit function theorem, this equation locally has a unique solution  $y_s(\lambda)$ , which can be written as:

$$y_s(\lambda) = \sum_{p \in \Upsilon} B_{s,p} \lambda^p + \mathcal{O}(|\lambda|^{\bar{p}+\epsilon}).$$

Note that the lowest value of  $p \in \Upsilon$  for which  $B_{s,p} \neq 0$  will generically be the minimum of the orders of the  $x_i(\lambda)$ , unless these all exceed 1. In that case, this lowest value of  $p$  generically equals 1, due to the presence of the term  $Q_{0,1}(0)\lambda^1$  in equation (4.15). Thus by definition of  $\hat{p}$ , we

indeed see that generically  $y_s(\lambda) \sim \lambda^{\bar{p}}$ . The coefficients  $B_{s,p} \in \mathbb{R}$  can iteratively be solved from the equation:

$$\alpha y_s(\lambda) + \sum_{\ell, m=0}^K Q_{\ell, m} \left( \bigoplus_{\sigma \in S_{k+1}^s} \mathbf{x}_{\sigma}(\lambda) \right) y_s^{\ell}(\lambda) \lambda^m + \mathcal{O}(|\lambda|^{\bar{p}+\epsilon}) = 0, \quad (4.16)$$

which is (4.15) applied to the solution branch  $(x_0(\lambda), \dots, x_k(\lambda), y_0(\lambda), y_1(\lambda))$ . We now want to show that:

$$y_0(\lambda) - y_1(\lambda) = \mathcal{O}(|\lambda|^{\bar{p}}), \quad (4.17)$$

for these unique solutions. We will do so by proving for all  $q \in \Upsilon$  with  $q < \bar{p}$  that:

$$[y_0]_{< q} = [y_1]_{< q} \implies [y_0]_{\leq q} = [y_1]_{\leq q}. \quad (4.18)$$

Note that for  $q = \min(p \mid p \in \Upsilon)$ , we have  $[y_0]_{< q} = [y_1]_{< q} = 0$ . Hence, iterated use of implication (4.18) indeed proves equation (4.17). To show that the statement in (4.18) holds, we subtract equation (4.16) for  $s = 1$  from the one for  $s = 0$ , which gives us:

$$\alpha(y_0(\lambda) - y_1(\lambda)) + \sum_{\ell, m=0}^K \sum_{s=0}^1 (-1)^s Q_{\ell, m} \left( \bigoplus_{\sigma \in S_{k+1}^s} \mathbf{x}_{\sigma}(\lambda) \right) y_s^{\ell}(\lambda) \lambda^m + \mathcal{O}(|\lambda|^{\bar{p}+\epsilon}) = 0. \quad (4.19)$$

Given  $q \in \Upsilon$  satisfying  $q < \bar{p}$ , let  $q^+$  denote the smallest element in  $\Upsilon$  such that  $q^+ > q$ , i.e.  $q^+$  is the 'next power' to consider. Note that  $q < \bar{p}$  means  $q^+ \leq \bar{p}$  exists. It follows that:

$$0 = \alpha([y_0(\lambda)]_{\leq q} - [y_1(\lambda)]_{\leq q}) + \sum_{\ell, m=0}^K \sum_{s=0}^1 (-1)^s Q_{\ell, m} \left( \bigoplus_{\sigma \in S_{k+1}^s} \mathbf{x}_{\sigma}(\lambda) \right) [y_s(\lambda)]_{< q}^{\ell} \lambda^m + \mathcal{O}(|\lambda|^{q^+}). \quad (4.20)$$

Here, we have used that:

$$Q_{\ell, m} \left( \bigoplus_{\sigma \in S_{k+1}^s} \mathbf{x}_{\sigma}(\lambda) \right) [y_s(\lambda)]_{\leq q}^{\ell} \lambda^m = Q_{\ell, m} \left( \bigoplus_{\sigma \in S_{k+1}^s} \mathbf{x}_{\sigma}(\lambda) \right) [y_s(\lambda)]_{< q}^{\ell} \lambda^m + \mathcal{O}(|\lambda|^{q^+}), \quad (4.21)$$

which is clear whenever  $\ell = 0$ ,  $\ell > 1$  or  $m > 0$ . For  $(\ell, m) = (1, 0)$  it holds because  $Q_{1,0}(0) = 0$ , so that  $Q_{1,0}$  has no constant term and hence:

$$Q_{1,0} \left( \bigoplus_{\sigma \in S_{k+1}^s} \mathbf{x}_{\sigma}(\lambda) \right)$$

is divisible by  $\lambda^r$  for  $r = \min(p \mid p \in \Upsilon)$ . We now assume  $[y_0(\lambda)]_{< q} = [y_1(\lambda)]_{< q}$  so that  $[y_s(\lambda)]_{< q} = [y_0(\lambda)]_{< q}$  for both choices of  $s$ . Using lemma 4.4, equation (4.20) becomes:

$$\begin{aligned} 0 &= \alpha([y_0(\lambda)]_{\leq q} - [y_1(\lambda)]_{\leq q}) \\ &+ \sum_{\ell, m=0}^K \sum_{s=0}^1 (-1)^s Q_{\ell, m} \left( \bigoplus_{\sigma \in S_{k+1}^s} \mathbf{x}_{\sigma}(\lambda) \right) [y_s(\lambda)]_{< q}^{\ell} \lambda^m + \mathcal{O}(|\lambda|^{q^+}) \\ &= \alpha([y_0(\lambda)]_{\leq q} - [y_1(\lambda)]_{\leq q}) \\ &+ \sum_{\ell, m=0}^K [y_0(\lambda)]_{< q}^{\ell} \lambda^m \sum_{s=0}^1 (-1)^s Q_{\ell, m} \left( \bigoplus_{\sigma \in S_{k+1}^s} \mathbf{x}_{\sigma}(\lambda) \right) + \mathcal{O}(|\lambda|^{q^+}) \\ &= \alpha([y_0(\lambda)]_{\leq q} - [y_1(\lambda)]_{\leq q}) \\ &+ \sum_{\ell, m=0}^K [y_0(\lambda)]_{< q}^{\ell} \lambda^m S_{\ell, m}(x(\lambda)) \prod_{\substack{i, j=0 \\ i > j}}^k (x_i(\lambda) - x_j(\lambda)) + \mathcal{O}(|\lambda|^{q^+}), \end{aligned} \quad (4.22)$$

for some polynomials  $S_{\ell, m}$ . As it is clear that:

$$\prod_{\substack{i,j=0 \\ i>j}}^k (x_i(\lambda) - x_j(\lambda)) = \mathcal{O}(|\lambda|^{\bar{p}}),$$

equation (4.22) simplifies to:

$$a([y_0(\lambda)]_{\leq q} - [y_1(\lambda)]_{\leq q}) = \mathcal{O}(|\lambda|^{\bar{q}}).$$

Using again the assumption that  $a \neq 0$ , this indeed gives  $[y_0(\lambda)]_{\leq q} = [y_1(\lambda)]_{\leq q}$ .

By induction, (4.17) holds true as outlined above. It follows that we may write:

$$y_0(\lambda) - y_1(\lambda) = E\lambda^{\bar{p}} + \mathcal{O}(|\lambda|^{\bar{p}+\epsilon})$$

for some  $E = B_{0,\bar{p}} - B_{1,\bar{p}} \in \mathbb{R}$ . We next want to show that  $E \neq 0$  generically. To this end, recall that  $B_{s,\bar{p}}$  can be solved for from equation (4.16). In fact, for fixed values of  $a \neq 0$  and the power series coefficients of each  $x_i(\lambda)$ , we may express  $B_{s,\bar{p}}$  as a polynomial in the coefficients of the various  $Q_{\ell,m}$ . Therefore, we may likewise express  $E = B_{0,\bar{p}} - B_{1,\bar{p}}$  as such a polynomial. Now, any polynomial on a finite dimensional vector space is either identically zero, or vanishes only on the complement of an open dense set. Therefore, the proof is complete if we can give at least one response function  $F$  for which  $E \neq 0$ . To this end, consider:

$$F(Y, \mathbf{X}; \lambda) = aY + P_{(k)}(\mathbf{X}). \quad (4.23)$$

Using lemma 4.5, we get:

$$\begin{aligned} 0 &= F\left(y_0(\lambda), \bigoplus_{\sigma \in S_{k+1}^0} \mathbf{x}_\sigma(\lambda); \lambda\right) - F\left(y_1(\lambda), \bigoplus_{\sigma \in S_{k+1}^k} \mathbf{x}_\sigma(\lambda); \lambda\right) \\ &= a(y_0(\lambda) - y_1(\lambda)) + P_{(k)}\left(\bigoplus_{\sigma \in S_{k+1}^0} \mathbf{x}_\sigma(\lambda)\right) - P_{(k)}\left(\bigoplus_{\sigma \in S_{k+1}^k} \mathbf{x}_\sigma(\lambda)\right) \\ &= a(y_0(\lambda) - y_1(\lambda)) + \prod_{\substack{i,j=0 \\ i>j}}^k (x_i(\lambda) - x_j(\lambda)) \\ &= a(y_0(\lambda) - y_1(\lambda)) + \left(\prod_{\substack{i,j=0 \\ i>j}}^k D_{i,j}\right) \lambda^{\bar{p}} + \mathcal{O}(|\lambda|^{\bar{p}+\epsilon}). \end{aligned} \quad (4.24)$$

Hence, for this particular choice of response function, we obtain:

$$E = -\frac{1}{a} \prod_{\substack{i,j=0 \\ i>j}}^k D_{i,j} \neq 0,$$

which shows that  $E$  is indeed generically non-vanishing.

Finally, equation (4.15) shows that the branch:

$$z(\lambda) = (x_0(\lambda), \dots, x_k(\lambda), y_0(\lambda), y_1(\lambda)) \quad (4.25)$$

is stable if  $x(\lambda)$  is stable for  $f_{(G)}^N$ , and if in addition  $a < 0$ . Since  $a = \partial F(0;0)/\partial y$ , this completes the proof. ■

**Remark 4.** The condition in theorem 4.2 that  $x(\lambda)$  is fully synchrony-breaking is essential. More precisely, it follows from remark 3 that if  $x_i(\lambda) = x_j(\lambda)$  for some distinct  $i, j$ , then the equations  $\dot{y}_0 = 0$  and  $\dot{y}_1 = 0$  give identical solutions  $y_0(\lambda)$  and  $y_1(\lambda)$ .

**Example 4.6.** The augmented hypernetwork depicted in figure 3 generically does not support a reluctant synchrony-breaking steady-state branch. Its core (shown in the grey box) is a fully symmetric three-cell network. It is known that this network only admits local synchrony breaking steady state branches for which  $x_i(\lambda) = x_j(\lambda)$  for a pair  $i \neq j$ , see [30]. Hence, all

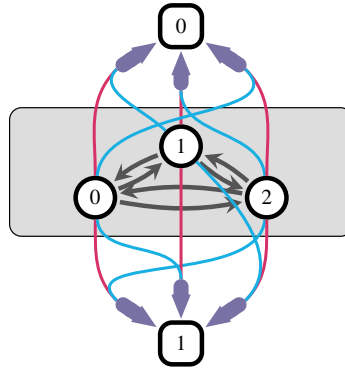


**Figure 3.** An augmented hypernetwork that generically does not support reluctant synchrony-breaking.

these branches are partially synchronous, and the conclusion of theorem 4.2 cannot be drawn. According to the previous remark, all generic solution branches in fact satisfy  $y_0(\lambda) = y_1(\lambda)$ .

**Remark 5.** Recall from remark 1 that we may generalize the definition of an augmented hypernetwork to allow only hyperedges between the two additional nodes and a subset  $\mathcal{S}$  of nodes of the same type of the core. It is clear that the results of theorem 4.2 still hold for this construction. More precisely, we then need a steady-state bifurcation branch in the core that has different components for the nodes in  $\mathcal{S}$ . We may then define the order of asynchrony as in definition 4.1, but comparing only states in  $\mathcal{S}$ . As in theorem 4.2, we will then generically have a steady-state bifurcation in a corresponding admissible vector field for the augmented hypernetwork, with the difference between the  $w$ -nodes growing in  $\lambda$  raised to the power of the order of asynchrony. Stability of this branch for the augmented hypernetwork can be guaranteed if the relevant branch for the core is stable.

## 5. More examples

In this section, we present three more examples that illustrate theorem 4.2.

**Example 5.1.** Consider the augmented hypernetwork shown in figure 4a. Its admissible ODEs are given by:

$$\begin{aligned}
 \dot{x}_0 &= G(x_0, x_1; \lambda), \\
 \dot{x}_1 &= G(x_1, x_0; \lambda), \\
 \dot{x}_2 &= G(x_2, x_2; \lambda), \\
 \dot{y}_0 &= F(y_0, (x_0, x_1), (x_1, x_2), (x_2, x_0); \lambda), \\
 \dot{y}_1 &= F(y_1, (x_0, x_2), (x_1, x_0), (x_2, x_1); \lambda),
 \end{aligned} \tag{5.1}$$

where  $F$  has the usual symmetry properties and where we assume each node to have a one-dimensional phase space. The grey box in figure 4a denotes the core of this hypernetwork, which is a disconnected, classical first-order network and whose dynamics corresponds to that of the  $x$ -variables in (5.1). Generically, a one-parameter bifurcation in an admissible system for the core is either given by the product of two saddle-nodes or by a pitchfork bifurcation. Only the latter of these involves a fully synchrony-breaking branch, and so we focus on that case, which we realize by choosing:

$$G(X_0, X_1; \lambda) = -X_0 - X_1 + \lambda X_0 - X_0^3. \tag{5.2}$$

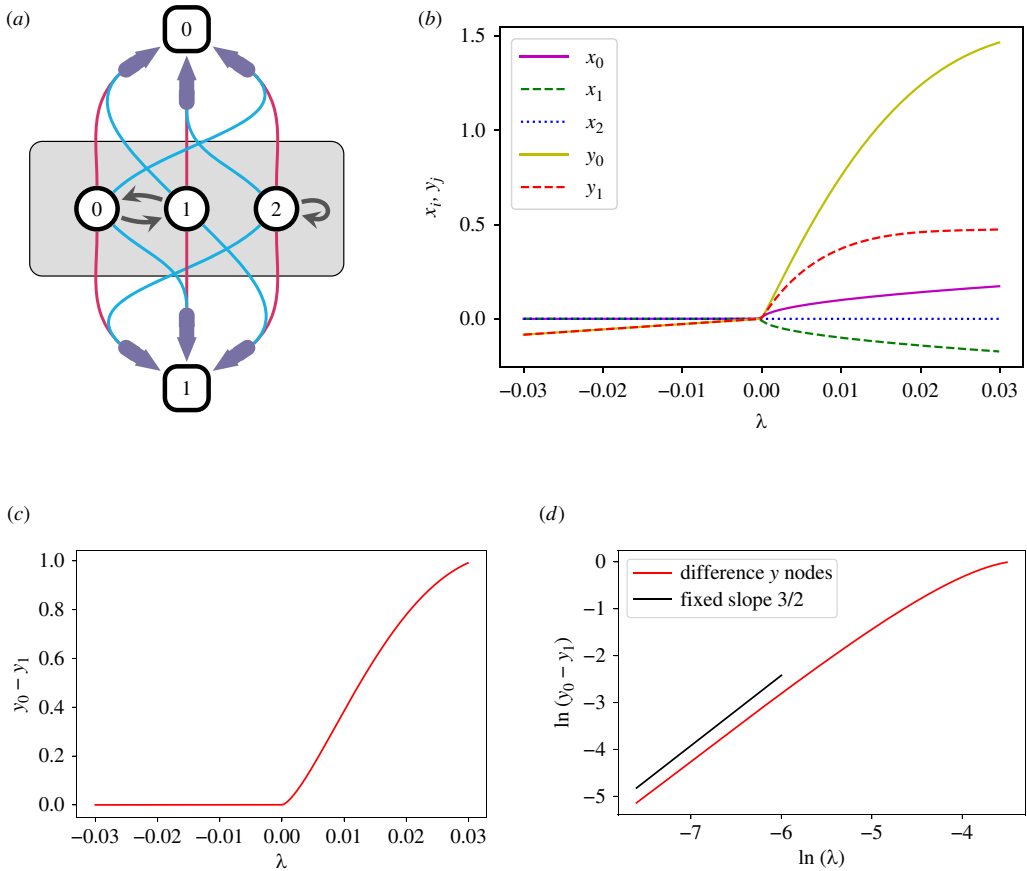


**Figure 4.** An augmented hypernetwork with a disconnected core together with the numerically obtained bifurcation diagram for a corresponding system of the form (5.1). (a) Depiction of the augmented hypernetwork whose core is shown within the grey box. We have left out self-loops corresponding to self-influence of each node. (b) The stable branches of a synchrony-breaking bifurcation. (c) The difference between the  $y$ -nodes along the stable branches. (d) A log–log plot of the difference between the  $y$ -nodes. The black line segment has fixed slope 3/2 for comparison, indicating that  $y_0(\lambda) - y_1(\lambda) \sim \lambda^{3/2}$ .

It follows that for  $\lambda < 0$ , the only (stable) steady-state branch is given by  $x_0(\lambda) = x_1(\lambda) = x_2(\lambda) = 0$ . For  $\lambda > 0$  we find (apart from some unstable branches) two stable, fully synchrony-breaking branches, given by:

$$x_0(\lambda) = -x_1(\lambda) = \pm\lambda^{1/2}, \quad x_2(\lambda) = 0.$$

For each of these two latter branches, we have:

$$x_2(\lambda) - x_0(\lambda) = \mp\lambda^{1/2}, \quad x_2(\lambda) - x_1(\lambda) = \pm\lambda^{1/2}, \quad x_1(\lambda) - x_0(\lambda) = \mp 2\lambda^{1/2},$$

from which we see that

$$\bar{p} = \frac{1}{2} + \frac{1}{2} + \frac{1}{2} = \frac{3}{2}.$$

Hence, for the choice of response function  $G$  given by (5.2), theorem 4.2 predicts the full system (5.1) to undergo a bifurcation where  $y_0(\lambda) - y_1(\lambda) \sim \lambda^{3/2}$  for  $\lambda > 0$ , for a generic choice of  $F$ .

A numerical investigation corroborates this result, see figure 4. These figures are obtained using Euler’s method for the system (5.1) with  $G$  given by equation (5.2) and where we use:

$$F(Y, (X_0, X_1), (X_2, X_3), (X_4, X_5); \lambda) = -5Y + 14\lambda - h(10X_0 - 12X_1) - h(10X_2 - 12X_3) - h(10X_4 - 12X_5)' \quad (5.3)$$

in which

$$h(x) = \sin(x) + \cos(x) - 1 = \sqrt{2}\sin\left(x + \frac{\pi}{4}\right) - 1. \quad (5.4)$$

This function  $F$  is chosen because it has non-vanishing Taylor coefficients of arbitrary order—to guarantee that the genericity conditions of theorem 4.2 hold—while also satisfying the required symmetry condition. We forward integrated the system (5.1) for each of 600 equidistributed values of  $\lambda \in [-0.03, 0.03]$ . For each fixed value of  $\lambda$ , integration was performed up to  $t = 5000$  with time steps of 0.1, and starting from the point  $(x_0, x_1, x_2, y_0, y_1) = (0.1, -0.2, 0.3, 0.4, 0.5)$ . For the log–log plot of figure 4d, we instead chose 600 values of  $\lambda \in [0.0005, 0.03]$ , such that the values of  $\ln(\lambda)$  are equidistributed.

**Example 5.2.** We next turn to the augmented hypernetwork depicted in figure 5a. The core of this hypernetwork, shown in the grey box, is an example of a classical (dyadic) network that itself shows reluctant synchrony-breaking. More precisely, admissible systems for this core are of the form:

$$\begin{aligned} \dot{x}_0 &= G(x_0, x_1, x_0; \lambda), \\ \dot{x}_1 &= G(x_1, x_2, x_0; \lambda), \\ \dot{x}_2 &= G(x_2, x_2, x_0; \lambda). \end{aligned} \quad (5.5)$$

These ODEs are special instances of those of the more general form:

$$\begin{aligned} \dot{x}_0 &= H(x_0, x_1, x_0, x_1, x_2; \lambda), \\ \dot{x}_1 &= H(x_1, x_2, x_0, x_1, x_2; \lambda), \\ \dot{x}_2 &= H(x_2, x_2, x_0, x_1, x_2; \lambda), \end{aligned} \quad (5.6)$$

obtained by setting  $H(x, y, z, u, v; \lambda) = G(x, y, z; \lambda)$ . Alternatively, one may think of (5.6) as denoting all admissible systems for a network obtained from the core in figure 5a by adding six additional arrows. The first three of these are from node 1 to all nodes in the core (including an additional self-loop for node 1), and are all of a single, new type. The last three are from node 2 to all nodes in the core, likewise all of one new type. The reason for adding these new arrow-types is that we can rigorously compute generic steady-state bifurcations in systems of the form (5.6), using centre manifold reduction. See Nijholt *et al.* [31] for a detailed exposition of the techniques used.

For the sake of this example, it is enough to know that in subsection 7.2 of Nijholt *et al.* [31] it is shown that the system (5.6) generically undergoes a steady-state bifurcation involving a synchrony-breaking branch:

$$\begin{aligned} x(\lambda) &= (x_0(\lambda), x_1(\lambda), x_2(\lambda)) \\ &= (D_0\lambda + \mathcal{O}(|\lambda|^2), D_1\lambda + \mathcal{O}(|\lambda|^2), D_1\lambda + \mathcal{O}(|\lambda|^2)), \end{aligned} \quad (5.7)$$

where

$$x_2(\lambda) - x_1(\lambda) = D_{2,1}\lambda^2 + \mathcal{O}(|\lambda|^3), \quad (5.8)$$

and with  $D_0, D_1, D_0 - D_1, D_{2,1} \neq 0$ . As this branch diverges from the synchrony space  $\{x_1 = x_2\}$  at only quadratic leading order, we may again speak of reluctant synchrony breaking. As opposed to the reluctant synchrony breaking we have considered in augmented hypernetworks though, the space  $\{x_1 = x_2\}$  is actually robust for systems of the form (5.6), and so for the special cases (5.5) as well. The synchrony-breaking branch (5.7) can furthermore take over stability from a fully synchronous one as  $\lambda$  increases through zero, see table 2.1 in Nijholt *et al.* [31]. We therefore predict such a bifurcation to occur in the special system (5.5) as well.

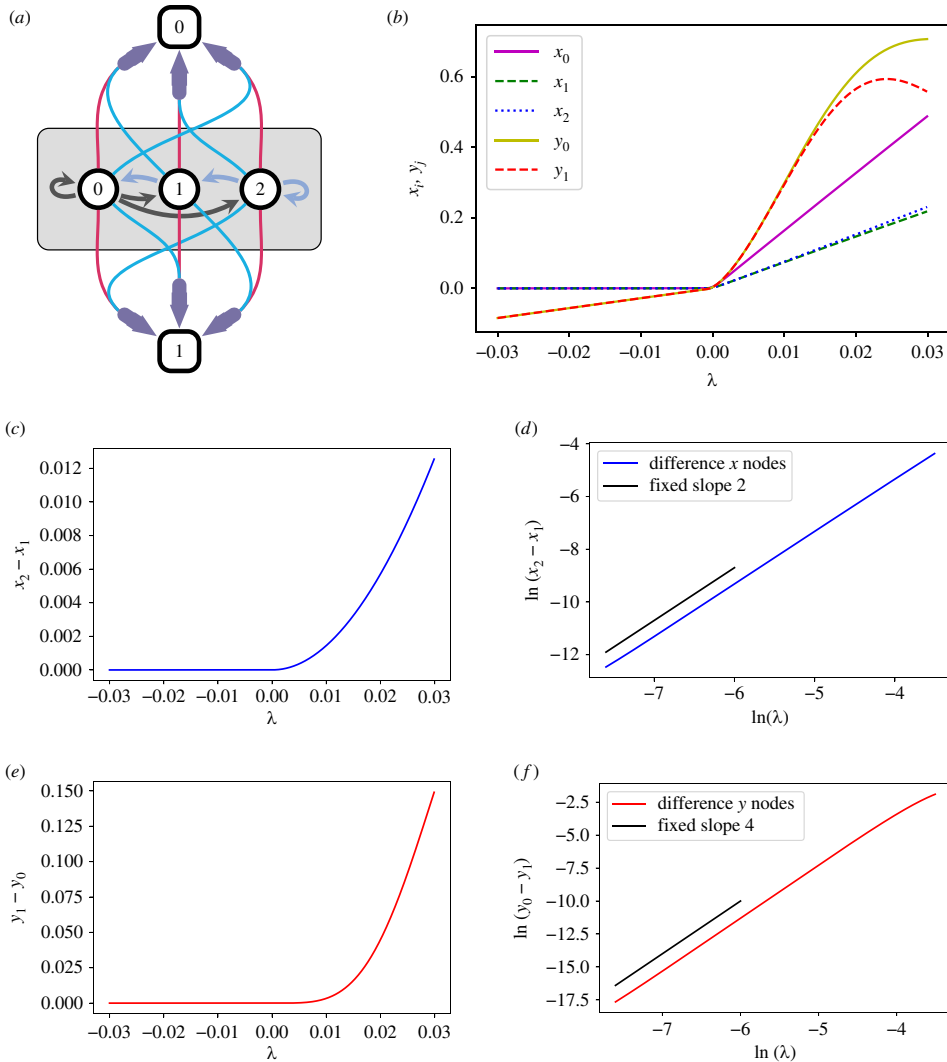


**Figure 5.** An augmented hypernetwork whose corresponding core system is of the form (5.5) and shows reluctant synchrony breaking itself together with the numerically obtained bifurcation diagram. (a) Depiction of the augmented hypernetwork. We have left out self-loops corresponding to self-influence of each node. (b) The stable branches of a synchrony-breaking bifurcation. (c) The difference between  $x_2$  and  $x_1$  along the stable branches. (d) A log–log plot of the difference between  $x_2$  and  $x_1$ . (e) The difference between the  $y$ -nodes along the stable branches. The black line segment has fixed slope 2 for comparison, indicating that  $x_2(\lambda) - x_1(\lambda) \sim \lambda^2$ . (f) A log–log plot of the difference between the  $y$ -nodes. The black line segment has fixed slope 4, which indicates that  $y_0(\lambda) - y_1(\lambda) \sim \lambda^4$ .

Figure 5 reveals that this is indeed the case. Figure 5b shows the components of the stable branches for the augmented hypernetwork of figure 5a. However, as the core is a subnetwork of its augmented hypernetwork, we see that the  $x$ -variables depend only on each other and so depict a bifurcation in the three-node system (5.5) as well. Figure 5b shows a reluctant separation happening between the nodes  $v_1$  and  $v_2$ , corresponding to the variables  $x_1$  and  $x_2$ , with figure 5c,d indicating this occurs as  $\sim \lambda^2$ .

It follows from (5.7) and (5.8) that we have

$$x_2(\lambda) - x_0(\lambda) \sim \lambda, \quad x_1(\lambda) - x_0(\lambda) \sim \lambda \quad \text{and} \quad x_2(\lambda) - x_1(\lambda) \sim \lambda^2,$$

so that

$$\bar{p} = 1 + 1 + 2 = 4.$$

By theorem 4.2, this implies that the augmented hypernetwork system generically exhibits the highly reluctant synchrony-breaking asymptotics:

$$y_0(\lambda) - y_1(\lambda) \sim \lambda^4.$$

The numerics in figure 5e,f corroborate this surprising asymptotics—see in particular the branches corresponding to the  $y$ -variables in figure 5b.

The details of the numerics are the same as for the previous example, except that time ran until  $t = 5000$  for figure 5b,c and e, and until  $t = 15000$  for figure 5d,f. The response function for the  $x$ -variables was chosen to be:

$$G(X_0, X_1, X_2; \lambda) = -0.55X_1 + 0.25X_2 + 1.5\lambda X_0 - 0.1X_0^2,$$

with  $F$  given by equations (5.3) and (5.4).

**Example 5.3.** Finally, we consider the augmented hypernetwork of figure 6a, which has as its core a classical feed-forward network with four nodes. More precisely, the nodes in the core evolve according to the ODEs:

$$\begin{aligned} \dot{x}_0 &= G(x_0, x_1, x_2; \lambda), \\ \dot{x}_1 &= G(x_1, x_2, x_3; \lambda), \\ \dot{x}_2 &= G(x_2, x_3, x_3; \lambda), \\ \dot{x}_3 &= G(x_3, x_3, x_3; \lambda). \end{aligned} \tag{5.9}$$

It is known that this system generically supports steady-state bifurcations in which stability passes from a fully synchronous branch to one in which:

$$x_0(\lambda) \sim \lambda^{1/4}, \quad x_1(\lambda) \sim \lambda^{1/2} \text{ and } x_2(\lambda), x_3(\lambda), x_2(\lambda) - x_3(\lambda) \sim \lambda,$$

see [29] and [32]. This unusually fast rate of synchrony breaking is also referred to as *amplification*. It follows that:

$$\bar{p} = \frac{1}{4} + \frac{1}{4} + \frac{1}{4} + \frac{1}{2} + \frac{1}{2} + 1 = \frac{11}{4},$$

so that theorem 4.2 predicts a reluctant steady-state branch with

$$y_0(\lambda) - y_1(\lambda) \sim \lambda^{\frac{11}{4}}.$$

This unusual growth rate is verified numerically in figure 6, which was obtained by numerically integrating the augmented system for:

$$G(X_0, X_1, X_2; \lambda) = 10X_1 - 20X_2 + 15\lambda X_0 - 100X_0^2,$$

and

$$F\left(Y, \bigoplus_{\sigma \in S_4^0} \mathbf{X}_\sigma; \lambda\right) = -0.01 \sum_{\sigma \in S_4^0} h(120X_{\sigma,1} + 40X_{\sigma,2} - 100X_{\sigma,3}) - 5Y - \lambda,$$

where  $\mathbf{X}_\sigma = (X_{\sigma,1}, \dots, X_{\sigma,4}) \in \mathbb{R}^4$  and with  $h$  given by equation (5.4).

Figure 6b shows the components of the stable branches, whereas figure 6c is a log–log plot of the difference of the  $y$ -components, for positive values of  $\lambda$ . In this latter picture, the dashed black line segment has fixed slope 11/4, indicating that indeed  $y_0(\lambda) - y_1(\lambda) \sim \lambda^{11/4}$ . For comparison we also plotted the dotted black line segment, which has fixed slope 10/4, and which does not fit as well for low values of  $\lambda$ . Both figures were made by forward integrating the vector field for the augmented system from the point:

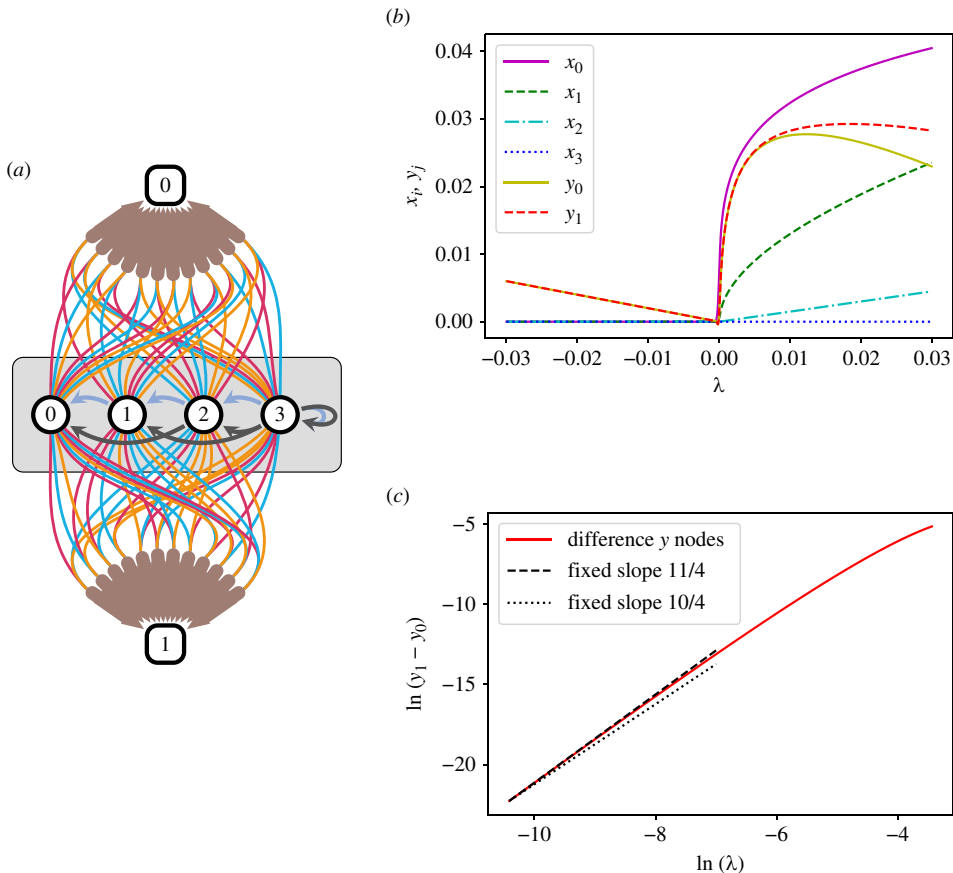


**Figure 6.** An augmented hypernetwork with a core consisting of a classical feed-forward network with four nodes, shown within the grey box. In contrast to the previous examples, for this hypernetwork we have  $k + 1 = 4$ , so that there are  $(k + 1)! = 24$  hyperedges of order  $k = 3$ . Also shown are numerically obtained bifurcation diagrams. (a) Depiction of the augmented hypernetwork. We have left out self-loops corresponding to self-influence of each node. (b) The stable branches of a synchrony-breaking bifurcation. (c) A log–log plot of the difference between the  $y$ -nodes. The dashed black line segment in the log–log plot has fixed slope  $11/4$ , whereas the dotted segment has fixed slope  $10/4$ .

$$(x_0, \dots, x_3, y_0, y_1) = (-0.001, -0.002, -0.003, -0.004, 0.001, 0.002)$$

in phase space, for various values of  $\lambda$  and with time steps of 0.1. For figure 6b, this was done up to  $t = 2000$  and with 600 equidistant values of  $\lambda \in [-0.03, 0.03]$ . For figure 6c, this was up to  $t = 20000$  and for 100 equidistant values of  $\ln(\lambda) \in [\ln(0.00003), \ln(0.03)]$ .

**Remark 6.** Example 5.2 shows that even classical (dyadic) networks may generically support reluctant synchrony breaking bifurcations. However, we are not aware of any method to design networks that, for instance, break synchrony up to some prescribed degree in  $\lambda$ . For hypernetworks, the augmented hypernetwork construction makes this design problem more tractable. In fact, we show below that one may construct hypernetworks that support generic reluctant synchrony breaking to arbitrarily high order.

To illustrate how one can create hypernetworks with an arbitrarily high order of reluctant synchrony breaking, we return to the five-node augmented hypernetwork of equation (2.1). In §2, we observed that the three-node core of this hypernetwork supports a steady-state branch in which  $x_i(\lambda) = D_i\lambda + \mathcal{O}(|\lambda|^2)$  for some mutually distinct  $D_i \in \mathbb{R}$ . Using the same notation as in §2, we expand the response function  $F$  for the  $y$ -nodes as:

$$\begin{aligned}
 & F(Y, (X_0, X_1), (X_2, X_3), (X_4, X_5); \lambda) \\
 & = aY + bX_0 + cX_1 + bX_2 + cX_3 + bX_4 + cX_5 + d\lambda \\
 & \quad + \mathcal{O}(\| (Y, X_0, \dots, X_5; \lambda) \|^2),
 \end{aligned} \tag{5.10}$$

and we recall that we found a reluctant steady-state branch in the augmented hypernetwork with asymptotics:

$$y_0(\lambda) = \frac{-(b+c)(D_0 + D_1 + D_2) - d}{a} \lambda + \mathcal{O}(|\lambda|^2), \tag{5.11}$$

and

$$y_1(\lambda) = \frac{-(b+c)(D_0 + D_1 + D_2) - d}{a} \lambda + \mathcal{O}(|\lambda|^2). \tag{5.12}$$

To this augmented hypernetwork, we can now add another node of the same type as the  $y$ -nodes, with corresponding variable  $y_2$ . We couple it to the nodes in the core in such a way that:

$$\dot{y}_2 = F(y_2, (x_0, x_1), (x_1, x_0), (x_0, x_0); \lambda). \tag{5.13}$$

The aforementioned branch of steady states is then supported by this larger hypernetwork as well, where in addition,

$$y_2(\lambda) = \frac{-(b+c)(D_0 + D_1 + D_0) - d}{a} \lambda + \mathcal{O}(|\lambda|^2), \tag{5.14}$$

as can be seen using [equation \(5.10\)](#). To summarize, we now have a branch where the three  $y$ -nodes satisfy:

$$\begin{aligned}
 y_0(\lambda) &= E_0 \lambda + \mathcal{O}(|\lambda|^2), \quad y_1(\lambda) = E_0 \lambda + \mathcal{O}(|\lambda|^2), \\
 y_2(\lambda) &= E_2 \lambda + \mathcal{O}(|\lambda|^2) \quad \text{and} \quad y_0(\lambda) - y_1(\lambda) \sim \lambda^p
 \end{aligned} \tag{5.15}$$

for some  $p > 1$  (in this particular case  $p = 3$ ). Moreover, from [equations \(5.11\), \(5.12\) and \(5.14\)](#) we see that  $E_0 \neq E_2$ , as  $D_0 \neq D_2$  by assumption.

We may now use the three  $y$ -nodes as the core for another augmented hypernetwork, say by adding two  $z$ -nodes of a new type (cf. [remark 5](#)). We also add a third  $z$ -node, precisely as we did with the third  $y$ -node. That is, we set:

$$\begin{aligned}
 \dot{z}_0 &= \tilde{F}(z_0, (y_0, y_1), (y_1, y_2), (y_2, y_0); \lambda), \\
 \dot{z}_1 &= \tilde{F}(z_1, (y_0, y_2), (y_1, y_0), (y_2, y_1); \lambda), \\
 \dot{z}_2 &= \tilde{F}(z_2, (y_0, y_1), (y_1, y_0), (y_0, y_0); \lambda),
 \end{aligned} \tag{5.16}$$

where  $\tilde{F}$  is a response function for the  $z$ -nodes. Just as before, we will then find:

$$\begin{aligned}
 z_0(\lambda) &= E'_0 \lambda + \mathcal{O}(|\lambda|^2), \quad z_1(\lambda) = E'_0 \lambda + \mathcal{O}(|\lambda|^2), \\
 z_2(\lambda) &= E'_2 \lambda + \mathcal{O}(|\lambda|^2) \quad \text{and} \quad z_0(\lambda) - z_1(\lambda) \sim \lambda^{p+2}
 \end{aligned} \tag{5.17}$$

for some generically non-zero  $E'_0, E'_2 \in \mathbb{R}$ . The new power  $p + 2$  follows from [theorem 4.2](#), as

$$y_2(\lambda) - y_0(\lambda) \sim \lambda, \quad y_2(\lambda) - y_1(\lambda) \sim \lambda, \quad y_0(\lambda) - y_1(\lambda) \sim \lambda^p, \tag{5.18}$$

which holds because  $E_0 \neq E_2$ . We may also argue that  $E'_0 \neq E'_2$  in precisely the same way that we argued that  $E_0 \neq E_2$ .

This shows that by iteratively growing the augmented hypernetwork, we may increase the order (in  $\lambda$ ) of reluctance of the reluctant steady-state branch. In other words, we may design hypernetworks with an arbitrarily high order of reluctant synchrony breaking. Concretely, our

example shows that we can arrange for  $p = 3, 5, 7, \dots$ . It is also clear from this construction that the resulting reluctant branch may be assumed stable.

## 6. Discussion

In von der Gracht *et al.* [16], the authors introduced a mathematical framework to capture higher-order interactions in network dynamical systems, thereby generalizing the analogous set-up for classical (dyadic) networks [22–24]. It is observed in von der Gracht *et al.* [16] that, unlike for dyadic networks, synchronization in these hypernetwork dynamical systems is governed by higher-order (nonlinear) terms in the equations of motion. This suggests that hypernetwork systems may display interesting phenomena that cannot be observed in dyadic networks. In particular, the authors of von der Gracht *et al.* [16] construct a hypernetwork system that shows numerical evidence of a bifurcation scenario in which two nodes break synchrony at an unusually high order in the bifurcation parameter.

In this paper, we provide a general method to construct hypernetwork systems displaying such ‘reluctant’ synchrony breaking, and we give a rigorous mathematical proof that these bifurcations occur generically in these systems. We also give an analytical expression for the order in the bifurcation parameter at which the synchrony breaking occurs.

Even though reluctant synchrony breaking is not impossible for dyadic networks, there is currently no understanding of what causes their (rare) occurrence. A method for constructing networks to achieve reluctant synchrony breaking is likewise lacking. In this paper, we show that this design problem is much more tractable for hypernetwork systems, and that the phenomenon appears to be significantly more common when higher-order interactions are present. This sheds new light on the role that such higher-order interactions play in various natural systems, and on their potential for applications in engineering.

In particular, we see interesting parallels with the concept of *homeostasis*. This term refers to the ability of living organisms to keep their internal states approximately stable when external conditions are changed. A well-known example is the ability of warm-blooded animals to regulate their body temperature across a wide range of environmental temperatures [33,34]. For dynamical systems with a distinguished input parameter  $\mathcal{I}$  and output function  $\mathcal{X}$ , an (infinitesimal) homeostasis point is an input parameter value  $\mathcal{I} = \mathcal{I}_0$  at which  $d\mathcal{X}/d\mathcal{I} = 0$ , with higher-order derivatives possibly vanishing too [35]. In our set-up, the output function is the difference between the states of two nodes at equilibrium, while the input parameter is a bifurcation parameter  $\lambda$ . Thus, reluctant synchrony breaking can be interpreted as a form of ‘synchrony homeostasis’. This phenomenon may well occur within living systems, as synchrony has been linked for instance to gene-regulatory processes [36] and memory formation in the brain [37]. Of course, such claims would have to be verified in the relevant biological systems. Nevertheless, it is striking that higher-order interactions can slow down desynchronization, perhaps to make a system more resilient to variations in external conditions.

**Data accessibility.** The code used to generate the numerical results is available online as part of the supplementary material online [38].

**Declaration of AI use.** We have not used AI-assisted technologies in creating this article.

**Authors’ contributions.** S.v.d.G.: conceptualization, formal analysis, investigation, methodology, project administration, resources, software, supervision, validation, visualization, writing—original draft, writing—review and editing; E.N.: conceptualization, formal analysis, investigation, methodology, project administration, resources, software, supervision, validation, visualization, writing—original draft, writing—review and editing; B.R.: conceptualization, formal analysis, investigation, methodology, project administration, resources, software, supervision, validation, visualization, writing—original draft, writing—review and editing.

All authors gave final approval for publication and agreed to be held accountable for the work performed therein.

**Conflict of interest declaration.** We declare we have no competing interests.

**Funding.** S.v.d.G. was partially funded by the Deutsche Forschungsgemeinschaft (DFG, German Research Foundation) - 453112019. E.N. was partially supported by the Serrapilheira Institute (Grant No. Serra-1709-16124). B.R. gratefully acknowledges the hospitality and financial support of the Sydney Mathematical Research Institute.

**Acknowledgements.** We thank Martin Golubitsky and Ian Stewart for enlightening discussions, as well as Tiago Pereira and Deniz Eroglu for helpful remarks on a draft of this manuscript.

## References

1. Ariav G, Polsky A, Schiller J. 2003 Submillisecond precision of the input-output transformation mediated by fast sodium dendritic spikes in basal dendrites of CA1 pyramidal neurons. *J. Neurosci.* **23**, 7750–7758. (doi:10.1523/JNEUROSCI.23-21-07750.2003)
2. Parastesh F, Mehrabbeik M, Rajagopal K, Jafari S, Perc M. 2022 Synchronization in Hindmarsh-Rose neurons subject to higher-order interactions. *Chaos* **32**, 013125. (doi:10.1063/5.0079834)
3. Neuhäuser L, Lambiotte R, Schaub MT. 2022 Consensus dynamics and opinion formation on hypergraphs. In *Higher-order systems* (eds F Battiston, G Petri), pp. 347–376. Cham, Switzerland: Springer International Publishing. (doi:10.1007/978-3-030-91374-8\_14)
4. Chatterjee S, Nag Chowdhury S, Ghosh D, Hens C. 2022 Controlling species densities in structurally perturbed intransitive cycles with higher-order interactions. *Chaos* **32**, 103122. (doi:10.1063/5.0102599)
5. Gibbs T, Levin SA, Levine JM. 2022 Coexistence in diverse communities with higher-order interactions. *Proc. Natl Acad. Sci. USA* **119**, e2205063119. (doi:10.1073/pnas.2205063119)
6. Pal PK, Anwar MS, Ghosh D. 2023 Desynchrony induced by higher-order interactions in triplex metapopulations. *Phys. Rev. E* **108**, 054208. (doi:10.1103/PhysRevE.108.054208)
7. Carletti T, Giambagli L, Bianconi G. 2023 Global topological synchronization on simplicial and cell complexes. *Phys. Rev. Lett.* **130**, 187401. (doi:10.1103/PhysRevLett.130.187401)
8. Anwar MS, Sar GK, Perc M, Ghosh D. 2024 Collective dynamics of swarmalators with higher-order interactions. *Commun. Phys.* **7**. (doi:10.1038/s42005-024-01556-2)
9. Nijholt E, Ocampo-Espindola JL, Eroglu D, Kiss IZ, Pereira T. 2022 Emergent hypernetworks in weakly coupled oscillators. *Nat. Commun.* **13**, 4849. (doi:10.1038/s41467-022-32282-4)
10. Mulas R, Kuehn C, Jost J. 2020 Coupled dynamics on hypergraphs: master stability of steady states and synchronization. *Phys. Rev. E* **101**, 062313. (doi:10.1103/PhysRevE.101.062313)
11. DeVille L. 2021 Consensus on simplicial complexes: results on stability and synchronization. *Chaos* **31**, 023137. (doi:10.1063/5.0037433)
12. Salova A, D'Souza RM. 2021 Analyzing states beyond full synchronization on hypergraphs requires methods beyond projected networks. Preprint. See <http://arxiv.org/pdf/2107.13712v1>.
13. Salova A, D'Souza RM. 2021 Cluster synchronization on hypergraphs. Preprint. See <http://arxiv.org/pdf/2101.05464>.
14. Nijholt E, DeVille L. 2022 Dynamical systems defined on simplicial complexes: symmetries, conjugacies, and invariant subspaces. *Chaos* **32**, 093131. (doi:10.1063/5.0093842)
15. Aguiar M, Bick C, Dias A. 2023 Network dynamics with higher-order interactions: coupled cell hypernetworks for identical cells and synchrony. *Nonlinearity* **36**, 4641–4673. (doi:10.1088/1361-6544/ace39f)
16. von der Gracht S, Nijholt E, Rink B. 2023 Hypernetworks: cluster synchronization is a higher-order effect. *SIAM J. Appl. Math.* **83**, 2329–2353. (doi:10.1137/23M1561075)
17. Battiston F, Cencetti G, Iacopini I, Latora V, Lucas M, Patania A, Young JG, Petri G. 2020 Networks beyond pairwise interactions: structure and dynamics. *Phys. Rep.* **874**, 1–92. (doi:10.1016/j.physrep.2020.05.004)

18. Porter MA. 2020 Nonlinearity + networks: a 2020 vision. In *Emerging frontiers in nonlinear science, nonlinear systems and complexity* (eds PG Kevrekidis, J Cuevas-Maraver, A Saxena), pp. 131–159, vol. 32. Cham, Switzerland: Springer International Publishing.
19. Torres L, Blevins AS, Bassett D, Eliassi-Rad T. 2021 The why, how, and when of representations for complex systems. *SIAM Rev.* **63**, 435–485. (doi:10.1137/20M1355896)
20. Bick C, Gross E, Harrington HA, Schaub MT. 2023 What are higher-order networks? *SIAM Rev.* **65**, 686–731. (doi:10.1137/21M1414024)
21. Boccaletti S, De Lellis P, del Genio CI, Alfaro-Bittner K, Criado R, Jalan S, Romance M. 2023 The structure and dynamics of networks with higher order interactions. *Phys. Rep.* **1018**, 1–64. (doi:10.1016/j.physrep.2023.04.002)
22. Golubitsky M, Nicol M, Stewart I. 2004 Some curious phenomena in coupled cell networks. *J. Nonlinear Sci.* **14**, 207–236. (doi:10.1007/s00332-003-0593-6)
23. Golubitsky M, Stewart I. 2006 Nonlinear dynamics of networks: the groupoid formalism. *Bull. New Ser. Am. Math. Soc.* **43**, 305–365. (doi:10.1090/S0273-0979-06-01108-6)
24. Field MJ. 2004 Combinatorial dynamics. *Dyn. Syst.* **19**, 217–243. (doi:10.1080/14689360410001729379)
25. Boldi P, Vigna S. 2002 Fibrations of graphs. *Discrete Math.* **243**, 21–66. (doi:10.1016/S0012-365X(00)00455-6)
26. DeVille L, Lerman E. 2015 Modular dynamical systems on networks. *J. Eur. Math. Soc.* **17**, 2977–3013. (doi:10.4171/jems/577)
27. Golubitsky M, Stewart I, Török A. 2005 Patterns of synchrony in coupled cell networks with multiple arrows. *SIAM J. Appl. Dyn. Syst.* **4**, 78–100. (doi:10.1137/040612634)
28. Aguiar MAD, Dias APS. 2014 The lattice of synchrony subspaces of a coupled cell network: characterization and computation algorithm. *J. Nonlinear Sci.* **24**, 949–996. (doi:10.1007/s00332-014-9209-6)
29. von der Gracht S, Nijholt E, Rink B. 2022 Amplified steady state bifurcations in feedforward networks. *Nonlinearity* **35**, 2073–2120. (doi:10.1088/1361-6544/ac5463)
30. Golubitsky M, Stewart I, Schaeffer DG. 1988 Singularities and groups in bifurcation theory: volume II. In *Applied mathematical sciences*, vol. 69. New York, NY: Springer.
31. Nijholt E, Rink B, Sanders J. 2019 Center manifolds of coupled cell networks. *SIAM Rev.* **61**, 121–155. (doi:10.1137/18M1219977)
32. Rink BW, Sanders JA. 2013 Amplified Hopf bifurcations in feed-forward networks. *SIAM J. Appl. Dyn. Syst.* **12**, 1135–1157. (doi:10.1137/120899649)
33. Golubitsky M, Stewart I. 2017 Homeostasis, singularities, and networks. *J. Math. Biol.* **74**, 387–407. (doi:10.1007/s00285-016-1024-2)
34. Wang Y, Huang Z, Antoneli F, Golubitsky M. 2021 The structure of infinitesimal homeostasis in input-output networks. *J. Math. Biol.* **82**, 62. (doi:10.1007/s00285-021-01614-1)
35. Golubitsky M, Stewart I. 2023 Dynamics and bifurcation in networks: theory and applications of coupled differential equations. In *Other titles in applied mathematics*, vol. 185. Philadelphia, PA: Society for Industrial and Applied Mathematics. (doi:10.1137/1.9781611977332)
36. Morone F, Leifer I, Makse HA. 2020 Fibration symmetries uncover the building blocks of biological networks. *Proc. Natl Acad. Sci. USA* **117**, 8306–8314. (doi:10.1073/pnas.1914628117)
37. Jutras MJ, Buffalo EA. 2010 Synchronous neural activity and memory formation. *Curr. Opin. Neurobiol.* **20**, 150–155. (doi:10.1016/j.conb.2010.02.006)
38. Nijholt E, von der Gracht S, Rink B. 2024 Supplementary material from: Higher order interactions lead to “reluctant” synchrony breaking. Figshare. (doi:10.6084/m9.figshare.c.7441723)